PURPOSE-LED
PUBLISHING™

TOPICAL REVIEW

Recent advances in GaN-based semiconductor lasers

To cite this article: Chunyu Zhao *et al* 2025 *Semicond. Sci. Technol.* **40** 073001

View the article online for updates and enhancements.

You may also like

Topical Review

Recent advances in GaN-based semiconductor lasers

Chunyu Zhao[1] , **Swee Tiam Tan**[1,2,*] **and Hilmi Volkan Demir**[1,3,*]

[1] LUMINOUS! Center of Excellence for Semiconductor Lighting and Displays, The Photonics Institute, School of Electrical and Electronic Engineering, School of Physical and Mathematical Sciences, School of Materials Science and Engineering, Nanyang Technological University, Singapore 639798, Singapore
[2] Kelip-kelip! Center of Excellence for Light Enabling Technologies, School of Energy and Chemical Engineering, Xiamen University Malaysia, Selangor, Darul Ehsan 43900, Malaysia
[3] Department of Electrical and Electronics, Department of Physics, and UNAM-Institute of Material Science and Nanotechnology and The National Nanotechnology Research Center, Bilkent University, Ankara TR-06800, Turkey

E-mail: sweetian.tan@xmu.edu.my and hvdemir@ntu.edu.sg

CrossMark

Abstract

III-nitride semiconductor lasers have made remarkable progress in recent years, particularly thanks to their ability to be tuned from the ultraviolet to the infrared. This comprehensive review explores the latest developments in GaN-based semiconductor lasers, with a specific focus on edge-emitting laser, vertical-cavity surface-emitting laser, photonic crystal or nanocrystal surface-emitting laser, and whispering gallery mode laser diodes. The review delves into each laser type's distinctive properties and potential applications, evaluating their performance while identifying current challenges. Finally, this review aims to shed light on challenges and prospects in GaN-based laser development.

Keywords: semiconductors, lasers, GaN

1. Introduction

III-nitride semiconductor laser diodes have been gaining increased interest in optical communication systems, data storage, solid-state lighting, and laser displays [1–3]. The band gap energy range in III-nitride based alloy can be precisely adjusted between 0.7 and 6.2 eV at room temperature by tuning its composition [4, 5]. As a result, GaN-based lasers theoretically can emit spectra covering a range from the ultraviolet (UV) to the infrared.

Furthermore, both GaN and its alloys with aluminum and indium exhibit a hexagonal wurtzite structure, and maintain a direct bandgap throughout the entire composition range spanning from AlN to InN. This characteristic renders them well-suited for laser diodes. Several factors significantly influence the performance of GaN-based lasers, such as the strong polarization field, substrate choice, quality of the thin films, and the quality of the crystal structure. To this end, this study conducts a synthesized review of GaN-based lasers.

The strong polarization field, inherent in GaN and its alloys, can affect the carrier distribution and recombination rates, which in turn impacts the laser's efficiency and threshold current. Figure 1 shows the hexagonal wurtzite GaN structure and major crystallographic planes. The crystal structure of GaN is hexagonal and lacks inversion symmetry along the [0001] crystallographic axis. Due to the difference in electronegativity between Ga and N, polar covalent bonds are formed in the compound. Nitrogen, being more electronegative, attracts

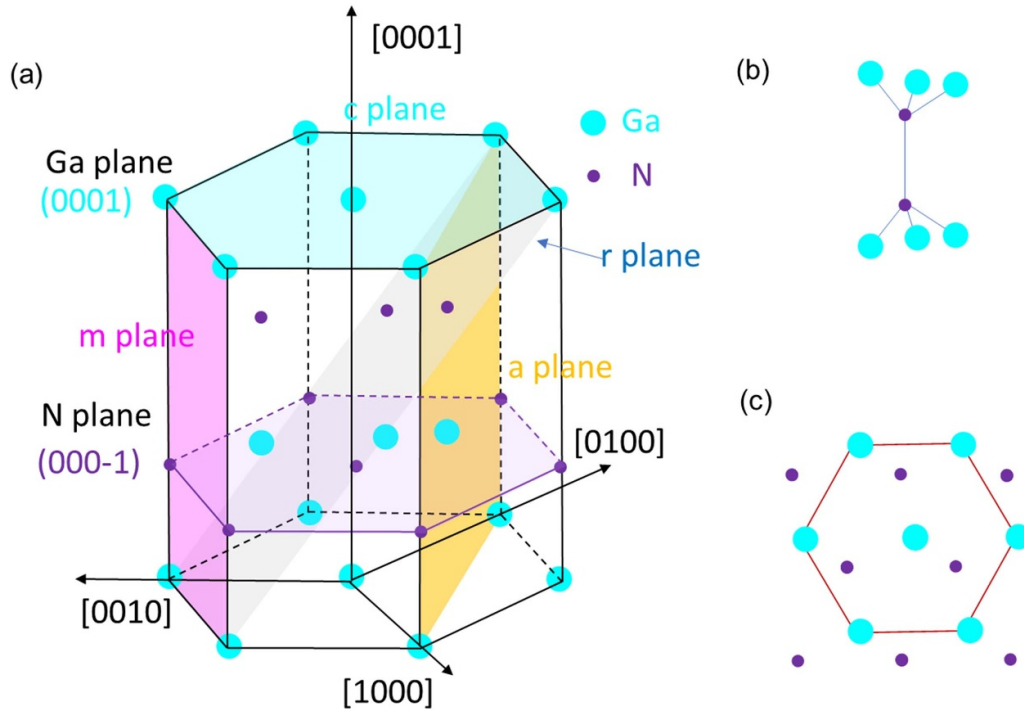* Authors to whom any correspondence should be addressed.

Figure 1. (a) Major crystallographic planes, (b) atomic structure with bonds configuration, and (c) top view of *c*-plane of hexagonal wurtzite GaN structure.

electrons more strongly, resulting in an uneven electron density distribution within the Ga-N bonds. This causes nitrogen to acquire a partial negative charge and gallium a partial positive charge. The resulting dipole moment within each Ga-N bond aligns across the entire crystal lattice, creating an overall dipole moment for the crystal. This alignment of dipole moments contributes to creating an electric field along the [0001] direction within the crystal due to its crystalline structure. Therefore, when growing GaN/InGaN quantum wells along the [0001] polar direction (*c*-plane) of the crystal, an electric field emerges across the InGaN layer. This electric field possesses the potential to compromise device performance due to the quantum-confined Stark effect (QCSE) [6, 7].

The choice of substrate is crucial for the growth and performance of GaN-based lasers, as different substrates offer varying advantages and challenges, impacting the quality, efficiency, and commercial viability of the resulting devices. Figure 2 shows the number of publications per year on GaN lasers grown on GaN, sapphire, and silicon (Si) substrates. GaN substrates provide the best lattice match and thermal properties for GaN laser growth. The major breakthroughs in high-power and long-lifetime blue GaN lasers on GaN substrates have been achieved after two decades of intensive research. Owing to the high cost and limited in wafer size associated with GaN substrates for homoepitaxial growth, GaN-based devices predominantly resort to heteroepitaxy on alternative substrate materials, such as sapphire and Si, and encounter a significant lattice mismatch issue [8–10]. A natural decline in the number of new publications of GaN lasers on GaN substrate since 2019 shown in figure 2 suggests a

shift in research focus towards the cost-effective substrates. Sapphire substrates are cost-effective and thermally stable but suffer from significant lattice and thermal mismatches with GaN. In comparison, Si offers cost advantages and potential for integration with existing electronics but faces significant lattice and thermal mismatch challenges. The substantial lattice mismatch gives rise to a high-density threading dislocations (TDs), impeding achieving the necessary high crystal quality for GaN materials [11–13]. There has been a significant increase in the number of publications on GaN lasers on Si substrates, surpassing those on sapphire and approaching those on GaN substrates.

High-quality thin films with minimal defects and uniform composition are essential for efficient light emission and long device lifetimes. In the 1990s, two pivotal breakthroughs in GaN semiconductor growth were the introduction of AlN [14] and GaN [9] nucleation layers, which enhanced the quality of GaN films and the achievement of p-type GaN [15–17]. These breakthroughs were crucial for making high-quality GaN films and paved the way for the fabrication of light-emitting devices. In 1996, Nakamura *et al* reported the groundbreaking achievement of introducing the inaugural pulsed current-injected GaN laser on sapphire substrates [18]. This marked a pivotal advancement in the evolution of GaN-based lasers, representing a notable milestone in semiconductor technology.

The successful commercialization of high power GaN-based edge-emitting lasers (EELs) emitting from blue to green has been realized through epitaxial growth on expensive *c*-plane GaN substrates [19]. Commercialized 455 nm blue and 525 nm green EELs have achieved optical output powers of
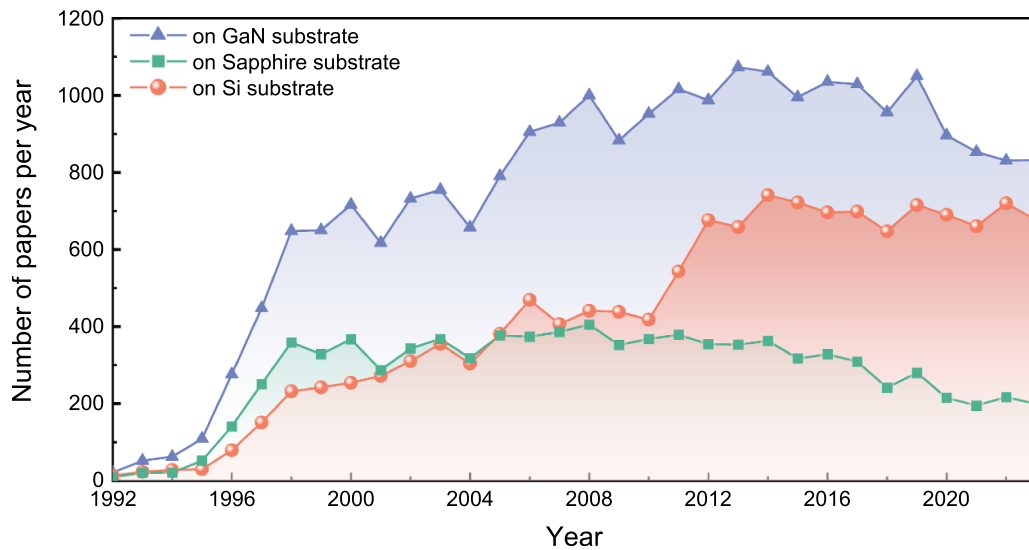
Figure 2. Number of papers published per year on GaN based lasers on GaN, sapphire and Si substates in the past decades (data taken from ISI Web of Science).

5.99 W and 1.97 W, respectively, with an estimated lifetime exceeding 30 000 h [20]. These GaN EELs have already been utilized in various applications, including displays and projectors. Recent achievements at laboratory scale have demonstrated the realization of GaN lasers on cost-effective and large-size Si substrates [10]. The substantial lattice mismatch of approximately 17% between GaN and Si has presented challenges leading to a high density of TDs [21]. These dislocations often act as non-radiative recombination centers, hindering the performance of GaN-based lasers on Si substrates. GaN-based EELs exhibit poor beam quality, resulting in a broader emission spectrum and increased beam divergence [22]. The endeavors for improving GaN laser performance and expanding their applications are well discussed in this paper.

Meanwhile, there is significant interest in GaN-based vertical cavity surface emitting lasers (VCSELs) owing to their precise beam control and noteworthy thermal stability [23]. The combination of short cavity length and low threshold current in GaN-based VCSELs leads to high-speed modulation, efficient power usage, and compact device designs. These characteristics make GaN-based VCSELs particularly advantageous for high-resolution imaging and optical communication applications, where performance and efficiency are critical. The commercialization of GaN-based VCSELs emitting at 445.9 nm (12 mW) and 514.9 nm (1.5 mW) on *c*-plane GaN substrates marks a significant technological advancement in the field [24]. It is essential to highlight that VCSELs may undergo a multi-transverse-mode operation when the lasing diameter is larger during high-power operations. Recently, green GaN-based VCSELs have been reported to exhibit a low threshold current density of 51.97 A cm^{-2} at an emission wavelength of 524 nm [25]. Recent research and development endeavors addressing challenges associated with high reflectance and low resistance distributed Bragg reflectors (DBRs) are discussed in this paper.

GaN-based photonic crystal surface-emitting lasers (PCSELs) [26], or nanocrystal surface-emitting lasers (NCSELs) [27] are gaining prominence owing to their capability to achieve single longitudinal and transverse mode oscillation in two dimensions. This unique feature enables them to achieve single-mode operation at high power levels by leveraging the band edge of the photonic band structure [28]. In addition to nitride-based optical microcavities of Fabry–Perot resonators and photonic crystal structures, there has been significant interest in whispering gallery mode (WGM) microdisk lasers [29]. GaN quantum dot (QD) -based WGM lasers have attracted more attention thanks to their enhanced optical properties. These microcavities have garnered attention for their diverse applications facilitated by high optical gain and a small mode volume [30].

A comprehensive review of the relevant literature will be especially helpful in synthesizing the key research insights and unveiling major research trends in developing GaN-based lasers. Although some studies have reviewed GaN-based UV lasers, semipolar InGaN lasers, and the application of GaN lasers in visible-light communications [31–33], a comprehensive examination focusing on material development and structural design for GaN-based lasers remains limited. Hence, this review article delves into the latest advancements across four distinctive categories of GaN laser structure. Spanning from conventional EELs to pioneering VCSELs, state-of-the-art PCSELs or NCSELs, and captivating WGM microcavity lasers, this discussion emphasizes material growth and structural design, providing an in-depth analysis of the technological progress and challenges within these domains. Through a detailed examination of recent breakthroughs in GaN-based lasers, we aim to provide valuable insights into the forefront of technological developments, paving the way for a deeper understanding of their potential applications and the future landscape of these semiconductor lasers.
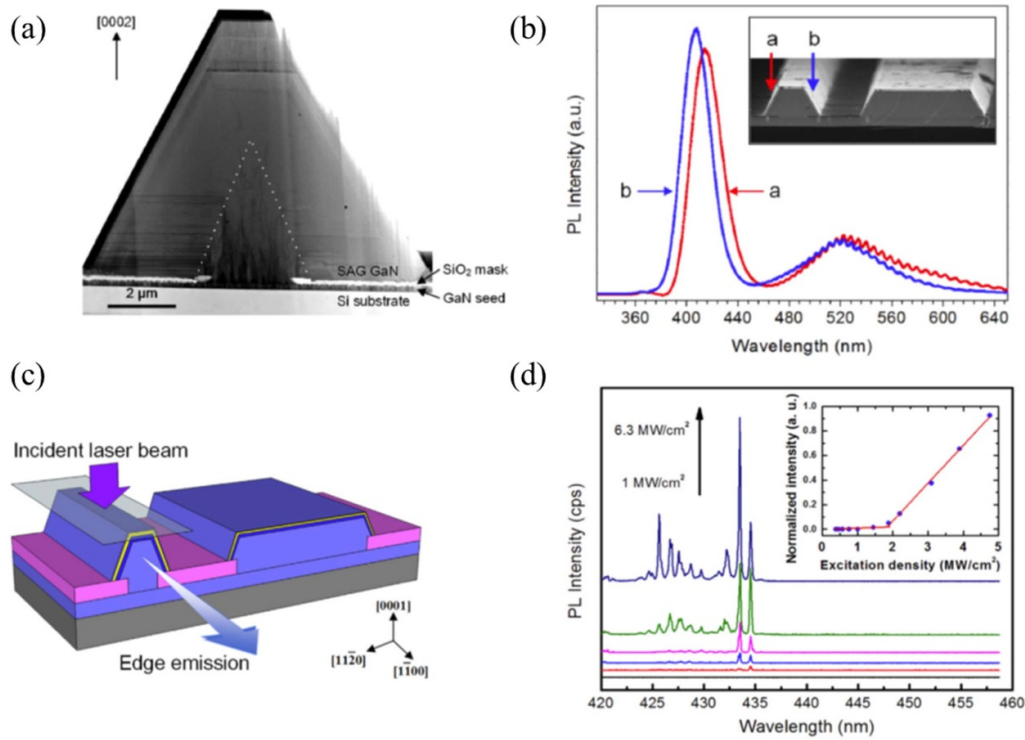
Figure 3. (a) Cross-sectional TEM bright-field image of the SAG laser diode cavity. (b) Photoluminescence spectra obtained on the two different side facets of the narrow strip. (c) Micro-photoluminescence spectra obtained on the two side facets of the thin stripe. (d) Edge emission spectra of a narrow stripe. Reprinted from [54], Copyright (2019), with permission from Elsevier.

2. EELs

GaN-based EELs feature a distinctive cavity structure, emitting light from the semiconductor's edge rather than the surface. The research began with the discovery of GaN stimulated emission, leading to room-temperature optically pumped lasing [34–37]. Nakamura *et al* then developed pulsed current-injected blue GaN EELs on sapphire using InGaN multiple quantum well (MQWs), achieving 215 mW at 2.3 A and 417 nm output [38, 39]. This progressed to room-temperature continuous wave (CW) operation with a lifetime exceeding 10 000 h at 20 °C [40]. Efforts with epitaxially laterally overgrowth (ELO) GaN or free-standing GaN substrates proved effective in enhancing GaN EELs' performance in CW operation [41–43]. This approach addressed crystal defect issues, impacting the efficiency and reliability of semiconductor lasers, allowing for the successful commercialization of GaN-based laser diodes through epitaxial growth on GaN substrates [19].

Significant efforts addressed challenges related to high indium content QWs, achieving progress in extending the emission wavelength of current-driven InGaN EELs to 531 nm [44–50]. Semipolar orientations demonstrated more minor piezoelectric polarization effects, leading to lower threshold current densities and improved laser efficiency. Especially for green GaN EELs grown on semipolar planes, such as (11–22), (20–2–1), and (20–21) planes, reports indicated substantial benefits, contributing to enhanced performance in terms of

lower threshold current densities and improved overall laser efficiency [51–53].

Considering cost-effectiveness, GaN-based EELs preferentially utilize *c*-plane GaN substrates over ELO and semipolar plane technologies. Notably, Nichia has successfully developed Watt-level GaN-based EELs that emit in the blue and green on *c*-plane GaN substrates, demonstrating mature processes and technologies for high-performance laser applications [20]. While the prevailing method for manufacturing GaN-based laser diodes relies on expensive GaN substrates, encountering challenges like non-uniformity in offcut angle and residual stress, researchers actively pursue more cost-effective solutions.

A promising approach involves growing GaN-based LDs on large-size, low-cost Si substrates. However, the growth of GaN on Si using metal-organic chemical vapor deposition (MOCVD) faces the issues of significant mismatch in both lattice constant (∼17%) and thermal expansion coefficient (∼56%) between GaN and Si [10, 21]. Efforts to enhance the quality of GaN on Si substrates have led to the achievement of stimulated emission only under optical pumping conditions at room temperature [54–56]. Figure 3(a) shows the transmission electron microscopy (TEM) micrograph of selective area growth (SAG) of semipolar InGaN/GaN MQWs laser diodes on the patterned GaN/AlN/Si (111) templates [54]. The spectra in figure 3(b) show that 530 and 416 nm peaks come from MQWs on the (0001) plane and along the left-side semipolar facet, respectively. Figures 3(c) and (d) illustrate the optically
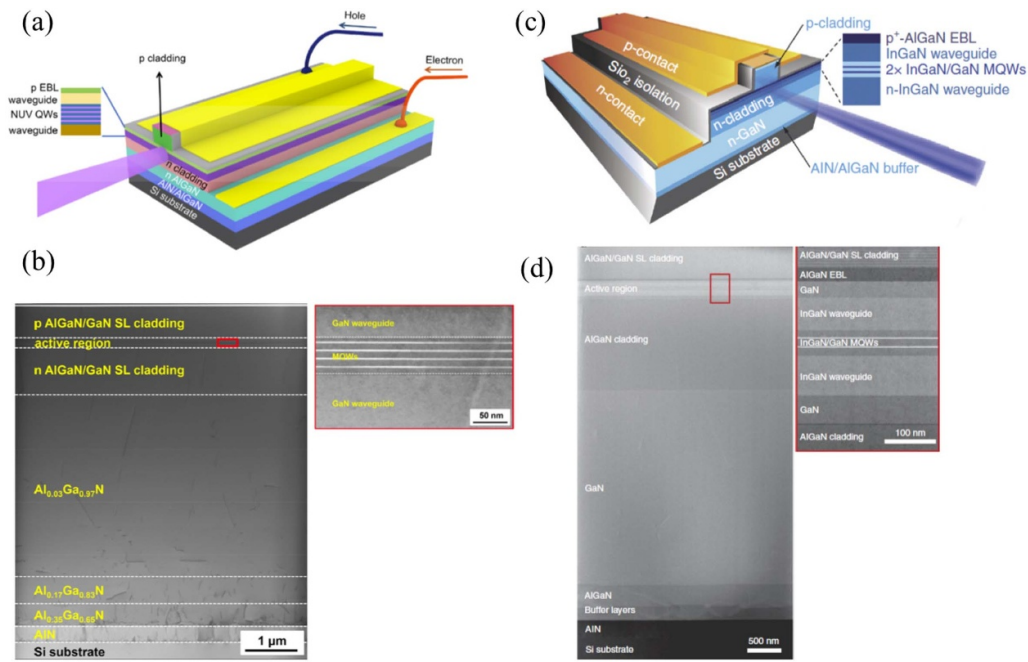
Figure 4. (a) Schematic architectures and (b) cross-sectional scanning TEM image of AlGaN-based NUV-LD structure grown on Si [57]. Reprinted with permission from [57]. Copyright (2018) American Chemical Society. (c) Schematic architectures and (d) cross-sectional scanning TEM image of InGaN/GaN QW blue laser diode structure grown on Si [58]. Reproduced from [58]. CC BY 4.0.

pumped lasing originating from the edge facet of the cavity, specifically emanating from the MQWs layers on the semipolar facets.

In 2016, Sun's team reported a groundbreaking achievement in developing room-temperature CW electrically injected blue–violet (413 nm) InGaN-based EELs on Si [10]. They employed an Al-composition step-graded AlN/AlGaN multilayer buffer to achieve a high-quality GaN film with a notably low TD density of 6×10^8 cm^{-2}. However, it is important to note that, despite this achievement, certain challenges persisted. The lasing threshold current density remained high at 4.7 kA cm^{-2}, and the operational voltage exceeded 8 V at room temperature, indicating limitations in the initial demonstration.

Subsequently, the same team demonstrated room-temperature CW electrically driven AlGaN-based near UV (NUV) (389 nm) [57] and blue (450 nm) [58] EELs grown on Si. Figures 4(a) and (c) show the typical architectures of EELs of AlGaN-based NUV-LD and InGaN/GaN QW blue laser diode structure grown on Si. By employing a precisely optimized Al composition step-downgraded AlN/AlGaN multilayer buffer, the well-defined interfaces of the InGaN/AlGaN QW active region are distinctly visible in figure 4(b). The TD density in the Al$_{0.03}$Ga$_{0.97}$N template was estimated to be as low as 6×10^8 cm^{-2}. To enhance the thin film quality of the InGaN/GaN quantum well blue laser diode on Si, Al-composition step-down-graded AlN/Al$_x$Ga$_{1-x}$N buffer layers were incorporated. The distinct interfaces for the individual layers are illustrated in figure 4(d).

The authors demonstrated room-temperature CW electrically injected InGaN EELs on a Si (100) substrate [59]. Figure 5

shows clear turning points at 320 and 350 mA, indicating the onset of lasing for the n-side ridge waveguide laser diode (nRW-LD) on Si (100). This report emphasizes compatibility with Si-based microelectronics and photonics platforms, underscoring the potential integration of GaN-based lasers with established Si technologies.

The advancement of highly efficient GaN EELs was propelled by their integration into augmented reality (AR) projection systems and virtual reality (VR) smart glasses and headsets [60]. To meet the demands for low energy consumption and a compact design, the preference is for GaN lasers with shorter cavities to decrease the threshold and enhance slope efficiency [61, 62]. Achieving uniformity and smoothness is the most challenging factor for GaN EELs with short cavities. The short cavity length amplifies the sensitivity of the laser to imperfections in the facets. An EEL with a cavity down to 75 μm was realized through a design incorporating one uncoated cleaved facet and one etched facet coated with a high-reflectivity dielectric DBR [63]. Figure 6 shows the schematic of the fabrication process. The laser successfully achieved lasing in the CW mode, demonstrating a threshold of 3.9 kA cm^{-2}. This indicates an efficient conversion of electrical power to optical output in the continuous operation of the laser device.

Recent advancements in GaN-based EELs from industry have focused on improving efficiency, power output, and miniaturization for various applications. High-power blue and green EELs on c-plane free-standing GaN substrates have been commercialized. Nichia reported a 455 nm blue EEL achieving 5.90 W under CW operation with 51.6% wall-plug efficiency (WPE) and a 525 nm green LD delivering
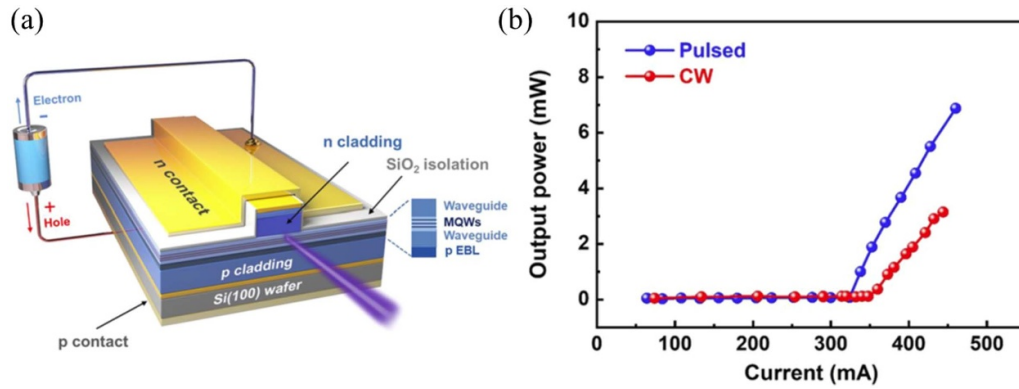
Figure 5. (a) Schematic architectures of nRW-LD on Si (100) substrate. (b) Light output power as a function of the pulsed and CW injection current at room temperature for nRW-LD on Si [59]. Reprinted with permission from [59]. Copyright (2020) American Chemical Society.
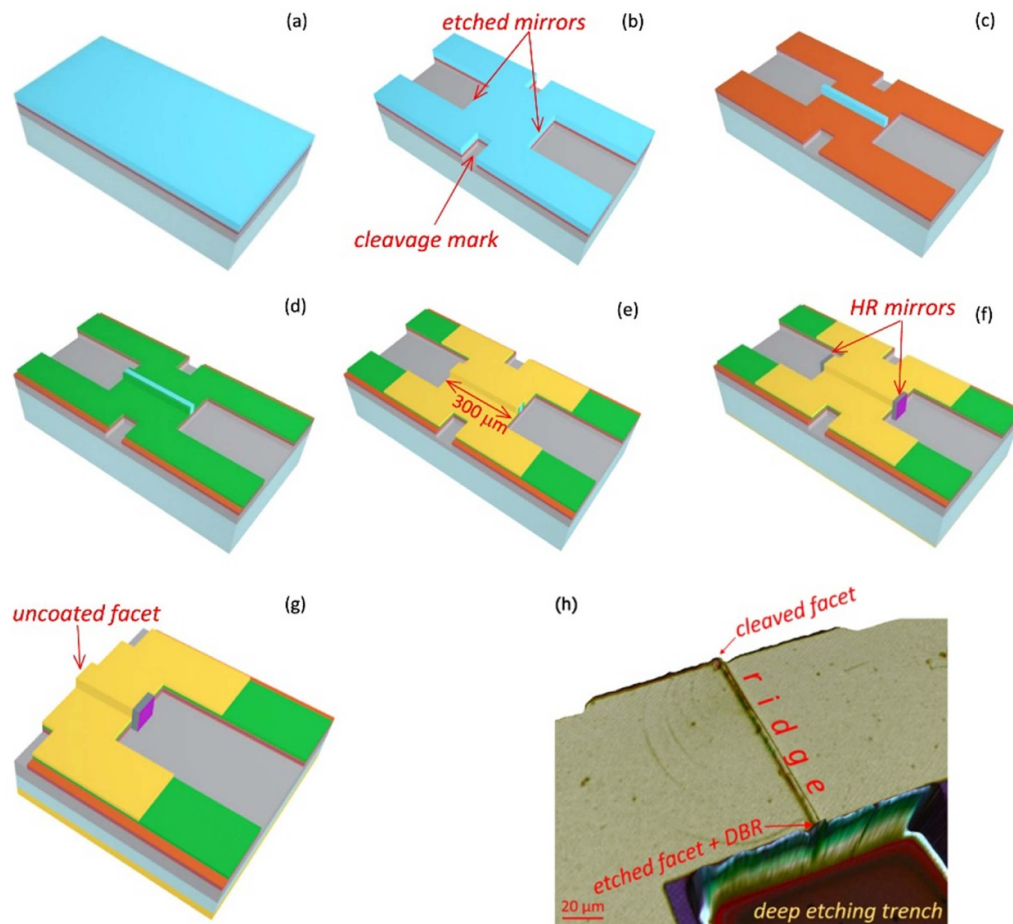

Figure 6. Schematics of the process flow (a)–(g) and confocal microscopy image (h) of a fully processed 100 μm long EEL. Reproduced from [63]. © IOP Publishing Ltd CC BY 3.0.

1.86 W at 1.9 A with a record 23.8% WPE [24]. Meanwhile, a GaN EEL grown on a Si substrate with a 100 μm cavity and cleaved facets has been reported by Kyocera Corporation [64]. The fabrication process of this EEL involved the application of the ELO technique. In this method, epitaxial layers were cleaved on the Si substrate by leveraging the inherent stress resulting from the variance in thermal

expansion coefficients. Subsequently, the cleaved dies were collectively transferred to a submount wafer using a junction down mount approach. Figure 7 shows a scanning electron microscopy (SEM) image of transferred dies on the submount wafer and light-current–voltage characteristics. The threshold current density for this laser device was 83 kA cm^{-2}.
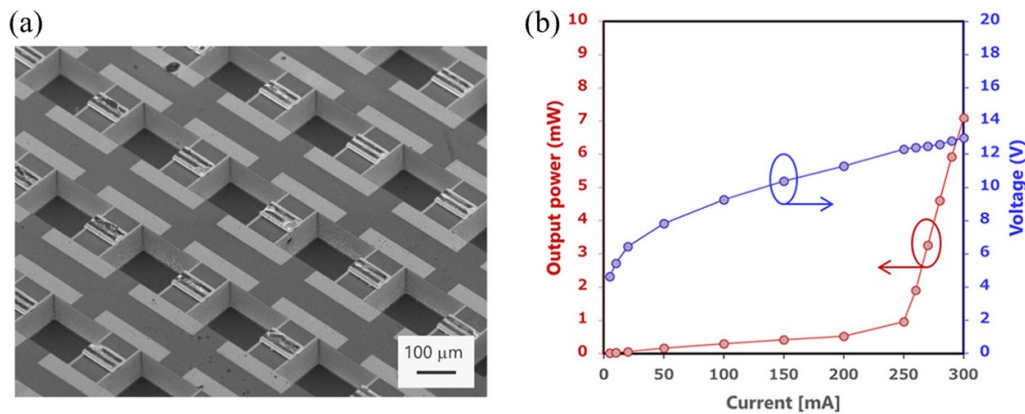
Figure 7. (a) SEM image of transferred dies on the sub-mount wafer and (b) light-current–voltage characteristics. Reproduced from [64]. CC BY 4.0.

In summary, GaN-based EELs have advanced significantly, featuring unique edge-emission from the semiconductor. GaN EELs have been successfully commercialized on GaN substrates, demonstrating high performance. Recent breakthroughs in growing GaN EELs on Si substrates have addressed lattice mismatch challenges, enabling room-temperature CW operation and integration with Si technologies. These innovations promise high-performance applications in AR and VR systems.

3. VCSELs

VCSEL is a semiconductor laser diode structure with laser beam emission perpendicular to the top surface [66]. In 1979, K. Iga published the pioneering work on GaInAsP/InP surface-emitting injection lasers, marking the inception of VCSEL technology [67–71]. GaAs-based VCSELs have since found extensive applications in data communication, material processing, and light detection and ranging, thanks to their compact size, low power consumption, high efficiency, and broad modulation bandwidth [72–74]. Despite the success of GaAs-based VCSELs, realizing GaN-based VCSELs posed more significant challenges due to difficulties in achieving high crystalline quality in GaN-based materials.

One of the primary obstacles in the development of GaN-based VCSELs is the formation of distributed DBRs. GaN has significant lattice mismatch with AlN and InN [75, 76], leading to high dislocation densities and increased electrical resistivity [77, 78]. Moreover, c-plane GaN devices encounter issues due to strong polarization field and the QCSE [79], complicating the achievement of efficient VCSELs. These factors collectively contribute to the complexity of achieving efficient VCSELs, emphasizing the need for innovative solutions to overcome these hurdles in advancing GaN-based VCSEL technology.

Initial attempts to develop GaN-based VCSELs focused on optically pumped devices. In 1995, Honda proposed the concept of a GaN-based VCSEL with highly reflective mirrors, utilizing AlN/AlGaN multilayer mirrors [80]. An optically pumped VCSEL of GaN as an active region sandwiched between 30-period $Al_{0.40}Ga_{0.60}N/Al_{0.12}Ga_{0.88}N$ Bragg reflectors was first published in 1996 [81]. The breakthrough in electrically pumped GaN-based VCSELs came in 2008 with the first CW laser operation reported using a hybrid microcavity with AlN/GaN and dielectric Ta_2O_5/SiO_2 DBRs [82]. CW laser action was achieved at a threshold injection current of 1.4 mA at an emission wavelength of 462.8 nm in the blue at 77 K. However, achieving room temperature lasing proved difficult due to the poor thermal conductivity of the sapphire substrate. VCSELs necessitate elevated current density, posing a challenge due to the associated increase in heat. The first room-temperature electrically pumped GaN-based VCSEL was reported in the same year [83]. Using laser lift-off, the sapphire substrate was detached. Subsequently, this VCSEL was mounted on a highly thermally conductive Si substrate through wafer bonding. The threshold current was 13.9 kA cm^{-2} at an emission wavelength of 414 nm.

Subsequent research focused on improving the performance of room-temperature lasing VCSELs, including via optimized GaN substrate [84], semi-polar GaN substrate [85, 86], ELO, curved mirrors [87, 88], and buried lateral index guides [89]. However, achieving a high-power output CW lasing at room temperature still presented a pending challenge. Further improvement of this weak output was hindered by the low reflectance and weak heat dissipation of the semiconductor DBR [90–92].

Various GaN-based DBRs, such as AlN/GaN [93–95], AlGaN/AlN [96–98], AlGaN/GaN [99, 100], and AlInN/GaN [97, 98], faced challenges in achieving both high reflectance and low resistance. Consequently, researchers have been exploring alternative approaches, such as employing all-dielectric DBRs like TiO_2/SiO_2 [101–105], Ta_2O_5/SiO_2 [106–108], and HfO_2/SiO_2 [109–111], to enhance reflectance. However, a hybrid cavity formed by combining a nitride
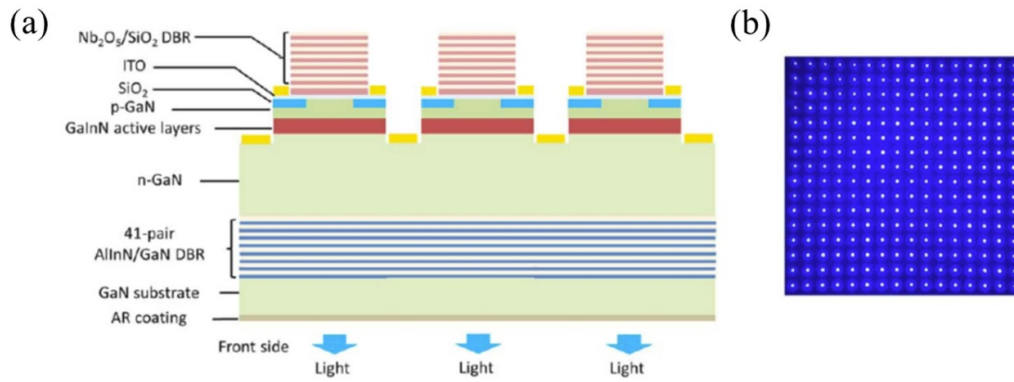
Figure 8. (a) Schematic diagram of the fabricated blue VCSEL array. (b) Emission image of the fabricated blue VCSEL array operated below the threshold [65]. Reproduced from [65]. © 2019 The Japan Society of Applied Physics. CC BY 4.0.
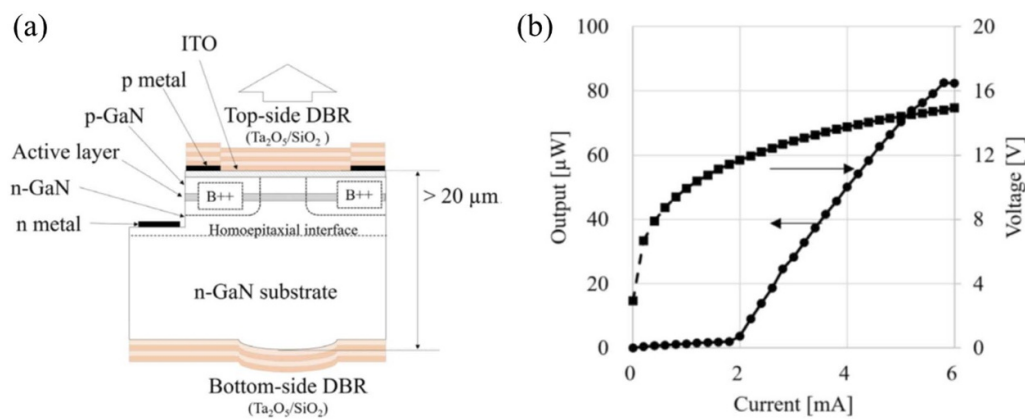

Figure 9. (a) Schematics of green VCSELs. (b) Current–voltage and current–output curves. Reproduced from [121]. © 2020 The Japan Society of Applied Physics. CC BY 4.0.

bottom DBR with a dielectric top DBR and utilizing all-dielectric DBRs all share the common problem of lower thermal resistance [112].

Okur *et al* introduced a design where an optical cavity was created on bottom high-reflectance dielectric DBRs embedded in GaN through ELO on a sapphire substrate [113]. Utilizing the ELO method, GaN-based VCSELs successfully achieved CW lasing at 446 nm at room temperature. The corresponding threshold current and maximum output power were measured at 8 mA and 0.9 mW, respectively [114].

In 2016, advancements led to CW operation lasing with an output power of 1.1 mW at 453.9 nm, leveraging the ELO technique to grow DBRs embedded in n-type GaN [115]. The novelty of this structure lies in that it utilizes the ELO technique to grow DBRs embedded in n-type GaN. Therefore, the device benefits from efficient heat extraction and DBRs with high reflectivity and a wide stopband. To further enhance output beyond milliwatt-class, a SiO$_2$-buried lateral index guide and long-cavity structure were implemented [89, 116, 117], resulting in a blue VCSEL array with a notable output power of 1.19 W [65]. The monolithic two-dimensional (2D) GaN-based VCSEL array, comprising 256 single elements arranged in a squared 16 × 16 matrix with a 100 μm pitch, was successfully fabricated, as shown in figure 8.

Despite these successes, GaN-based VCSELs primarily demonstrated emission in the blue region. The development of longer wavelengths, especially for green light, has faced challenges, often referred to as the 'green gap' [118]. GaN-based materials pose difficulties in forming green light emission devices due to the higher indium content, which can lead to an increased density of defects and dislocations.

Nichia achieved room-temperature pulsed lasing for a green GaN-based VCSEL, producing an output power of 0.80 mW at a laser emission wavelength of 503 nm [119]. A decade later, following the first report of electrically injected pulsed lasing VCSELs, Nichia achieved room-temperature CW operation of milliwatt-class single-mode blue and green VCSELs by replacing the double dielectric DBR with a hybrid DBR structure [120]. Sony employed a semipolar GaN substrate to cultivate InGaN/GaN MQWs, successfully realizing lasing for a green VCSEL at 515 nm. However, the threshold current density remains relatively large at 14.4 kA cm^{-2} [121], as shown in figure 9.

Recently, GaN-based VCSELs have demonstrated wavelengths covering most of the 'green gap,' as shown in figure 10 [122]. The threshold of these low-threshold green VCSELs is in the sub-milliampere range, attributed to the utilization of a QD based active region. An AlN layer served as the current confinement layer, and an electroplated
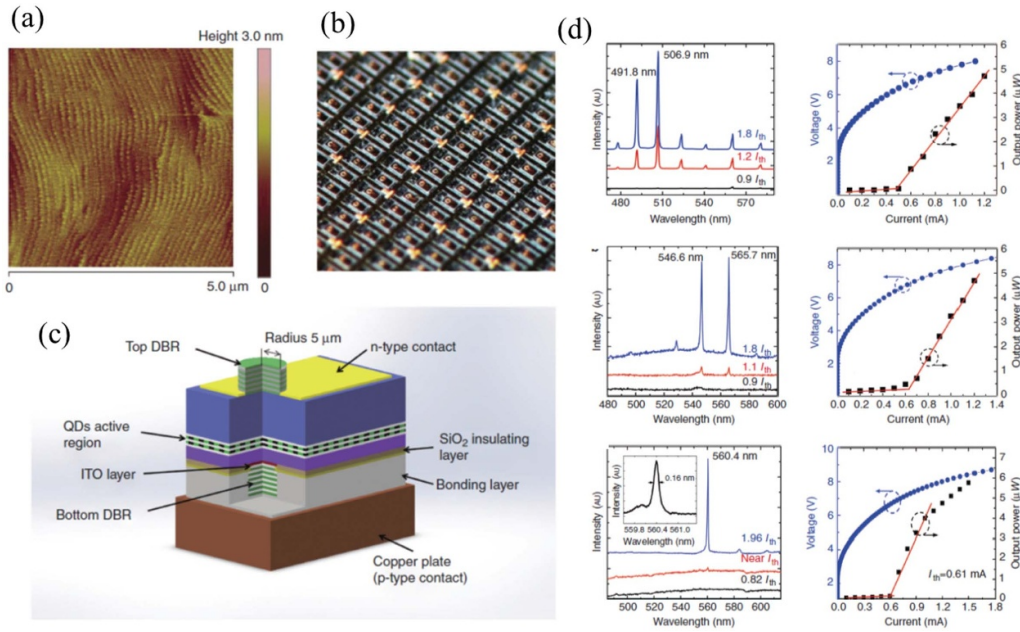
Figure 10. (a) AFM image of uncapped InGaN QD layer. (b) Schematic structure of the GaN-based VCSEL with a vertical current-injection configuration and QD active region. (c) Photograph of the VCSEL array. (d) Room-temperature CW lasing spectra at different current levels (left) and the corresponding voltage–current–light output characteristics (right) of three samples with varying lengths of the cavity [122]. Reproduced from [122], with permission from Springer Nature.

copper plate replaced traditional metal bonding to enhance heat dissipation. The outcomes offer crucial insights for achieving high-performance GaN-based VCSELs. Notably, room-temperature CW lasing was successfully achieved with the lowest threshold current density recorded at 51.97 A cm^{-2}, emitting at 524 nm [25].

Overall, the development of GaN-based VCSELs has progressed significantly, addressing various challenges through innovative solutions. The successful commercialization of GaN-based VCSELs, which emit blue and green light with milliWatt power levels on *c*-plane GaN substrates, represents a major technological breakthrough in the field [24]. Despite ongoing hurdles, particularly in achieving efficient green emission, continuous improvements in material quality, thermal management, and DBR design are paving the way for high-performance GaN-based VCSELs across a broader wavelength spectrum.

4. PCSELs or NCSELs

Photonic crystals, initially introduced in 1987 by Yablonovitch and John [123, 124], consist of periodic structures with alternating refractive indices. A defining characteristic of photonic crystals lies in their capacity to control the emission and transmission of light by delineating permissible and restricted photonic energy bands and establishing the dispersion relation between photon energy and wave vector [125–127]. GaN-based lasers incorporating photonic crystals can be categorized into two types. The first type involves confining light within a single defect of a nanofabricated 2D photonic crystal, commonly known as a photonic crystal defect mode cavity laser [128, 129]. The second type is PCSEL or NCSEL.

Photonic crystal defect mode cavity lasers confine light within a single defect of a nanofabricated 2D photonic crystal. These lasers benefit from high Q-factors and small modal volumes, which enhance stimulated emission of cavity polaritons, resulting in a potent Purcell effect and low lasing thresholds [130–133]. However, the development of GaN-based photonic crystal defect mode cavity lasers faces significant challenges, including limited well-controlled etching techniques and the difficulties associated with low-damage etching. These issues hinder precision lithography, particularly because GaN devices emit at shorter wavelengths compared to GaAs-based devices emitting at longer wavelengths.

In 2005, Choi *et al* achieved the first blue laser using a GaN-based photonic crystal defect mode cavity [134]. The L7 photonic crystal membrane nanocavity, featuring seven absent holes along the Γ–*K* direction of the triangular lattice photonic crystal structure, was created through a photoelectrochemical (PEC) etching technique combined with optimized low-power etching methods [135–140]. The investigation focused on the Q-factors of the mode in relation to the ratio between the lattice constant and the radius of an air hole, revealing that a smaller ratio is preferable for achieving robust spatial coupling between the mode and the active region. This preference arises because a photonic crystal with a smaller lattice constant effectively prevents the maximum intensity displacement into the air dielectric. However, this design exhibited limited output power, restricting its applicability in high-power scenarios.

The second type, PCSELs, employs multidirectional distributed feedback (DFB) near the band edges within 2D

photonic crystal structures. In-plane coupling is induced by specific band edges through DFB, causing diffraction in perpendicular directions [141–143]. This is a consequence of the first-order Bragg diffraction for modes above the light line. Consequently, PCSELs can effectively achieve expansive single-mode operation across large areas, generating high output power with narrow divergence angles through surface emission [144–146].

In 2008, a significant advancement in GaN-based PCSELs utilized air holes retained overgrowth combined with nanofabrication [26]. The process included creating a GaN/air periodic structure on n-GaN substrate through electron beam lithography and dry etching. Adding a SiO$_2$ layer at the bottom of air holes prevented excess GaN growth. Overcoming challenges, low-pressure MOCVD growth ensured uniform air hole arrangement. Capping top of the air holes prevented dislocations during regrowth, yielding a well-defined GaN-based PCSEL. Resonant light coupling occurred when the in-plane wave vector aligned with photonic bands, reaching a threshold at 67 kA cm^{-2} under pulsed current operation. However, the low refractive index contrast in III-nitride materials and the lack of reliable techniques for forming impeccable nanostructures within GaN limit the strength of the 2D photonic-crystal resonant effect.

S Noda's group has pioneered a novel nanofabrication technique that eliminates the need for a SiO$_2$ block layer, a significant achievement realized over a decade after the research mentioned above [28]. This was carried out to prevent the introduction of significant structural disorders, which can lead to scattering loss and material impurities that may impact the device's performance. To incorporate air holes beneath a GaN film with a remarkably even surface, the growth conditions were fine-tuned to promote lateral growth and mitigate mass-transport phenomena exclusively. Ultimately, this optimized regrowth and nanofabrication process successfully realized a GaN-based PCSEL with a double-lattice photonic crystal structure. These breakthroughs have allowed a GaN PCSEL's successful operation with a remarkably low threshold current density of 2–3 kA cm^{-2} and a high output power of approximately 320 mW.

In addition to the completed nanofabrication and regrowth process, alternative photonic-crystal fabrication methods exist. One such method involves utilizing a mass-transport phenomenon to form crystallographic facets on the inner walls of voids [147]. This technique observed lasing action at 406 nm for a photonic crystal lattice constant of 162.5 nm. The threshold current density, ranging from 9.7 to 28.6 kA cm^{-2}, depends on the size of the p-contact electrode. Unfortunately, this mass-transport approach suffers from the drawback of compromising the uniformity of the GaN/air structure, and coherent 2D oscillation is unattainable due to the square lattice's inability to sustain the necessary 2D optical coupling.

Furthermore, the GaN PCSEL was explored by investigating a combination of DBRs and GaN-based photonic crystal structures [148]. These lasers demonstrate lasing action under optical pumping at room temperature, with a threshold pumping energy density of approximately 3.5 mJ cm^{-2}. The laser emits a dominant wavelength of 424.3 nm with a linewidth of about 1.1 Å. The normalized frequency of the investigated photonic crystal lasing wavelength corresponds to the calculated Brillouin-zone boundary provided by the 2D hexagonal-lattice photonic crystal patterns [148]. GaN-based photonic crystal nanobeam cavities, fabricated using electron-beam lithography and focused-ion beam (FIB) milling, achieved a high quality factor of 740 [149].

In 2020, Mi's group developed all-epitaxial surface-emitting green lasers utilizing GaN nanostructures [27]. This approach achieved dislocation-free GaN nanocrystal arrays using a selective area epitaxy growth technique. These diodes utilize GaN nanostructures and stand out for their absence of dislocations, achieved through efficient strain relaxation. Figure 11 shows the design of InGaN NCSEL diodes operating in the green wavelength. The fabrication involved employing nano-hole Ti masks with a diameter of approximately 180 nm and a lattice constant of 250 nm arranged in triangular lattices. This intricate design of NCSELs was actualized through e-beam lithography and a reactive ion dry-etching technique. The active region, positioned on semipolar planes, encompasses multiple InGaN quantum disks and a unique AlGaN shell structure designed to reduce the QCSE and suppress surface recombination significantly. The hexagonally shaped nanocrystals are arranged in a triangular lattice with a spacing of approximately 30 nm, and the lattice constant is 250 nm. This nanocrystal design facilitates both in-plane and out-of-plane coupling.

The reciprocal lattice of the photonic crystal structure, with its six equivalent G'' points, induces in-plane coupling through the Bragg grating vectors. Additionally, there is out-of-plane coupling between the six G'' points and the G point, resulting in vertical surface emission. The InGaN NCSEL diodes operating at a wavelength of approximately 523 nm, the device exhibits a threshold current of around 400 A cm^{-2} and an output power of ∼12 mW at an injection current density of ∼1 kA cm^{-2} under CW operation. This approach holds great promise for advancing the field of surface-emitting laser diodes with all-epitaxial structures.

In recent advancements, GaN-based epitaxial nanowire photonic crystal structures have demonstrated significant progress in UV lasing. One notable study reported lasing at a wavelength of 367 nm with an impressively low threshold of 7 kW cm^{-2}, equivalent to approximately 49 μJ cm^{-2} [150]. Additionally, strong light emission under direct electric current injection was observed at around 383 nm with a threshold current of approximately 0.2 mA [151]. This achievement not only marks a significant milestone in the development of UV PCSEL but also lays the groundwork for the development of surf lasers with customizable lasing wavelengths. This advancement holds promise for a wide range of applications such as high-resolution imaging and advanced communication technologies, due to the tunability and efficiency of these nanowire photonic crystal structures.

In summary, GaN-based lasers utilizing photonic crystals have advanced significantly, particularly in photonic crystal defect mode cavity lasers and PCSELs. While offering high
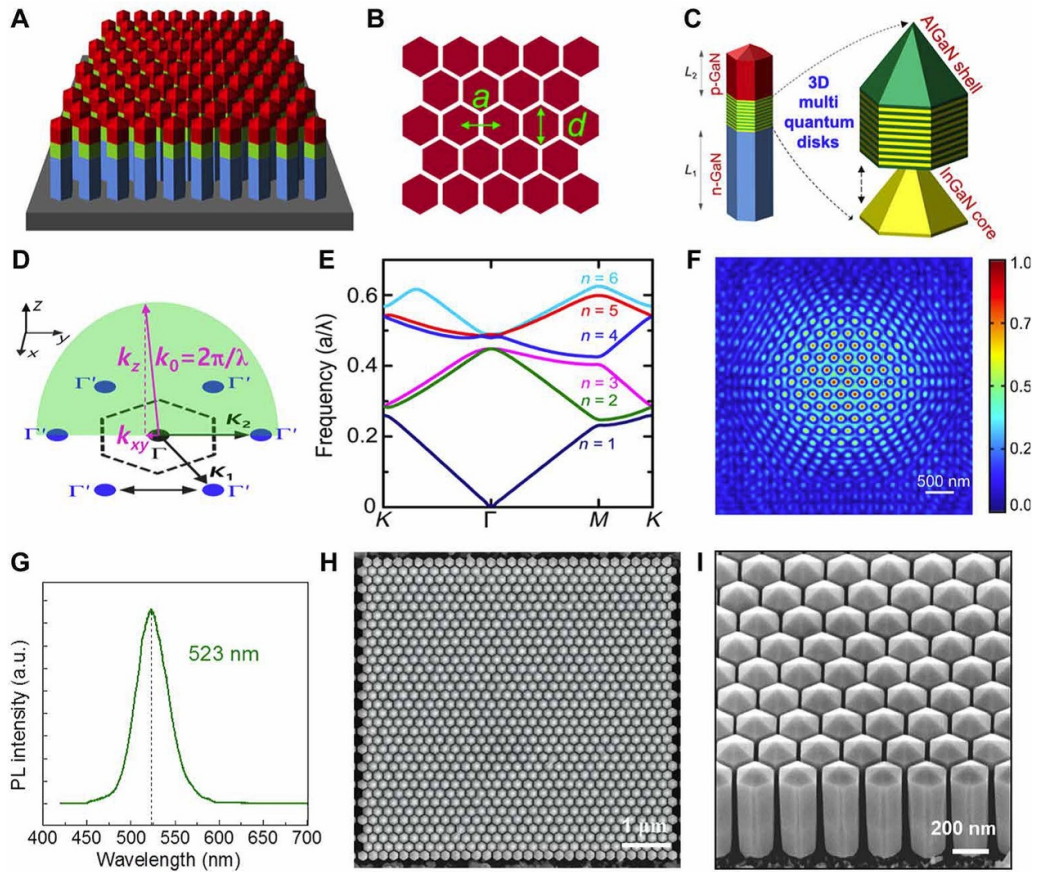
Figure 11. Design of InGaN NCSEL diodes operating in the green wavelength. (A) Schematic of the InGaN nanocrystal arrays for the surface-emitting laser diode. (B) Diameter and lattice constant of the nanocrystals denoted as *d* and *a*, respectively. (C) Schematic of the InGaN/AlGaN nanowire heterostructure. (D) The reciprocal lattice of a photonic crystal structure has six equivalent G! points. (E) Calculated photonic band structure. (F) The electric field profile of the band edge mode (523 nm). (G) Photoluminescence spectrum of an InGaN/AlGaN calibration sample showing spontaneous green emission [27]. From [27]. Reprinted with permission from AAAS.

Q-factors and low thresholds, defect mode lasers struggle with etching challenges and limited output power. PCSELs or NCSEL achieve high output power through multidirectional feedback but face limitations from low refractive index contrast. Recent innovations, such as dislocation-free GaN nanostructures, have further improved performance, indicating a promising future for laser technology.

5. WGM lasers

WGM lasers utilize the whispering gallery effect, in which light waves are confined within a circular (or spherical) structure through total internal reflection. This effect allows the continuous propagation of light along the circumference of the microdisk (or spherical structure), generating resonant modes and facilitating laser operation. III-nitride microdisk lasers are distinguished by their capacity to confine and amplify light in a compact volume. They offer advantages such as high optical gain, a minor mode volume, and low lasing thresholds. As a result, these attributes make them suitable for a variety of applications in photonics and telecommunications.

GaN-based microdisk lasers have attracted considerable attention due to their exceptional characteristics [152–155]. A significant advancement occurred with the introduction of PEC etching, allowing for the creation of undercut structures for GaN on sapphire substrates [156–160]. This breakthrough paved the way for successfully demonstrating CW blue lasing at room temperature. Remarkably, a very low threshold of 300 W cm^{-2} was achieved in GaN microdisks containing InGaN QWs, as highlighted by Tamboli *et al* [161].

Creating a mushroom structure is essential in the fabrication of GaN-based microdisk lasers. In addition to employing PEC etching of the InGaN superlattice sacrificial layer [162], an alternative strategy involves using a KOH (potassium hydroxide) solution to etch the oxidized AlInN sacrificial layer [163]. Moreover, the transfer of III-nitride grown on sapphire substrates to Si represents an alternative method for creating a mushroom structure [164, 165], as illustrated in figure 12, depicting the schematic of the transfer process [166]. The GaN-based microdisk laser grown on sapphire can also undergo transfer onto a polyethylene terephthalate substrate [167]. While these approaches offer an advantage in utilizing
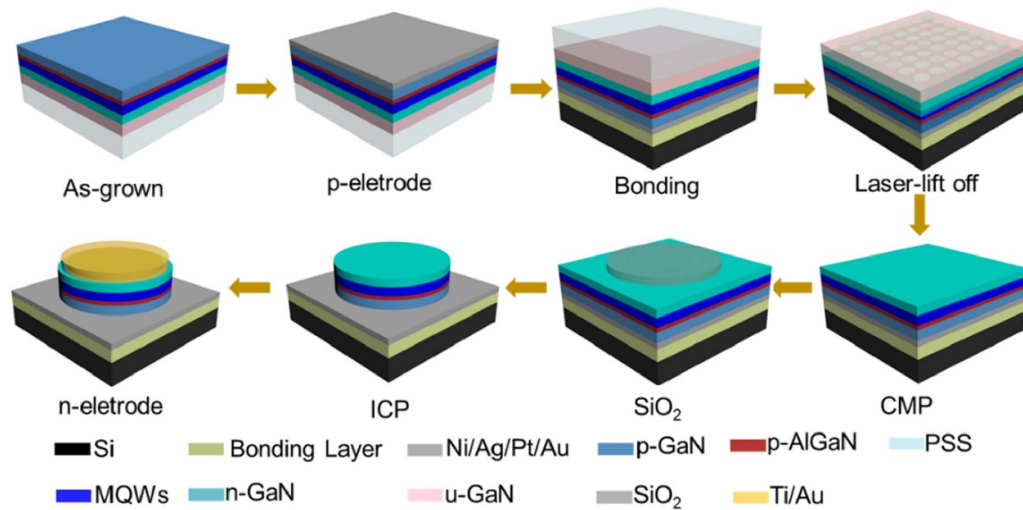
Figure 12. Schematic diagrams illustrating the process flow of InGaN-based microdisk integrated on Si (100). Reprinted with permission from [166]. © 2022 Optica Publishing Group.

the high crystalline quality of GaN on sapphire. However, these complex processes can introduce challenges of potential reliability issues and restrictions on the performance of GaN microdisk lasers.

In addition to the intricate etching methods involving the InGaN superlattice or AlInN sacrificial layer, another notable strategy for achieving undercut GaN microdisks is based on utilizing GaN material grown directly on a Si substrate. In 2006, Choi *et al* successfully demonstrated micro-lasers based on pivoted GaN microdisk arrays on Si substrates [168]. The process involved growing GaN films on a Si substrate and patterning using photolithography and dry etching techniques. A small Si pedestal was created to provide mechanical support for the microdisk through a wet etching process, effectively removing the Si surrounding and underneath the microdisks.

T. Guillet's group expanded on these findings by showcasing microdisk lasers operating under room-temperature pulsed optical pumping across a wide spectral range from 275 to 470 nm, achieving a high-quality factor exceeding 1000 [169, 170]. Additionally, alternative strategies have been explored to enhance the performance of GaN microdisk lasers. These include using floating asymmetric circle and circle GaN microdisks and employing floating large-size GaN microdisks with gratings [171]. T. Wang successfully achieved room-temperature CW lasing from an InGaN microdisk on Si, producing emission wavelengths of 442, 493, and 522 nm [172, 173].

However, further development of GaN microdisk lasers has been encountering severe high threshold problems. A method to overcome this problem is the growth of QDs as active regions.

Recent advancements in GaN QD WGM lasers have drawn significant global attention due to their promising potential in various applications. The integration of QDs within WGM structures enhances carrier confinement and recombination efficiency, leading to improved temperature stability and reduced lasing thresholds. The utilization of GaN QDs presents inherent advantages over QWs [174–176]. The three-dimensional confinement characteristic of QDs, serving as the gain medium in nitride-based microdisk lasers, theoretically offers benefits such as low-threshold operation and high optical gain [177, 178]. The combination of QDs and WGM lasers exemplifies a cutting-edge approach in III-nitride semiconductor lasers, offering a path towards innovative solutions and future technological breakthroughs.

GaN/AlN QD based microdisk lasers have set a noteworthy record Q-factor of 7,300, boasting exceptionally low lasing thresholds that reach as low as 60 W cm^{-2} [179]. Another remarkable milestone has been achieved with a record-low lasing threshold of 0.28 mJ cm^{-2} in GaN microdisks featuring InGaN QDs and an impressive Q-factor of 6,600 [180]. Furthermore, substantial progress has been made by Lau's group in the development of ultra-low threshold green InGaN QD microdisk lasers grown directly on Si substrates [181]. Figure 13(a) illustrates the epitaxial configuration of microdisk lasers on Si. Figure 13(b) shows a cross-sectional TEM image showcasing the as-grown sample featuring a three-stacked InGaN/GaN QD structure. Figure 13(c) presents a detailed TEM image of the three-stacked QD active region, highlighting the presence of uniformly aligned QD. Figure 13(d) shows photoluminescence spectra at room temperature. The microdisk laser fabrication process is shown in figure 14. At an excitation power density of 0.4 kW cm^{-2}, the peak wavelength from the as-grown QDs on the Si is observed at 545 nm, accompanied by a full-width-at-half- maximum (FWHM) of 43 nm. The threshold is below 100 W cm^{-2} at the emission wavelength of 522 nm.

In a distinct accomplishment, Hu's group demonstrated that GaN micro-rings incorporating InGaN QDs and fragmented
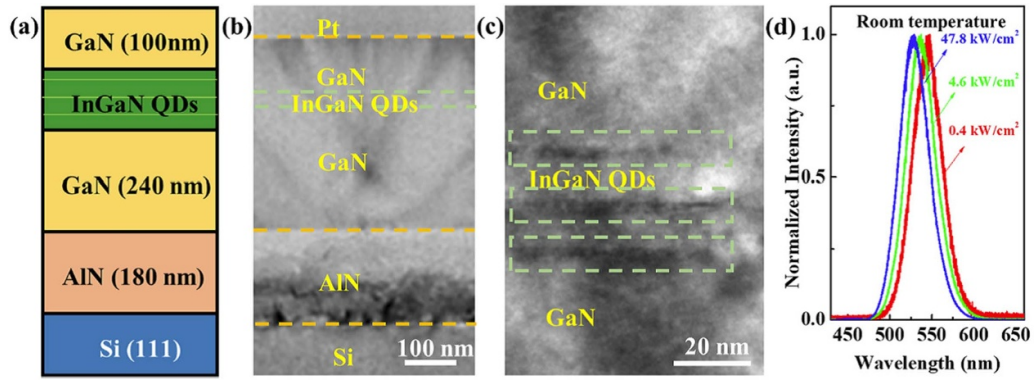
Figure 13. (a) Schematic illustration of the epitaxial structure of material in the disk region; cross-sectional TEM image of (b) the microdisk structure and (c) the three-stacked InGaN QDs; (d) room-temperature photoluminescence spectra of the as-grown QD microdisk lasers on Si substrates at increasing excitation power densities from 0.4 to 47.8 kW cm^{-2}. Reprinted from [181], with the permission of AIP Publishing.
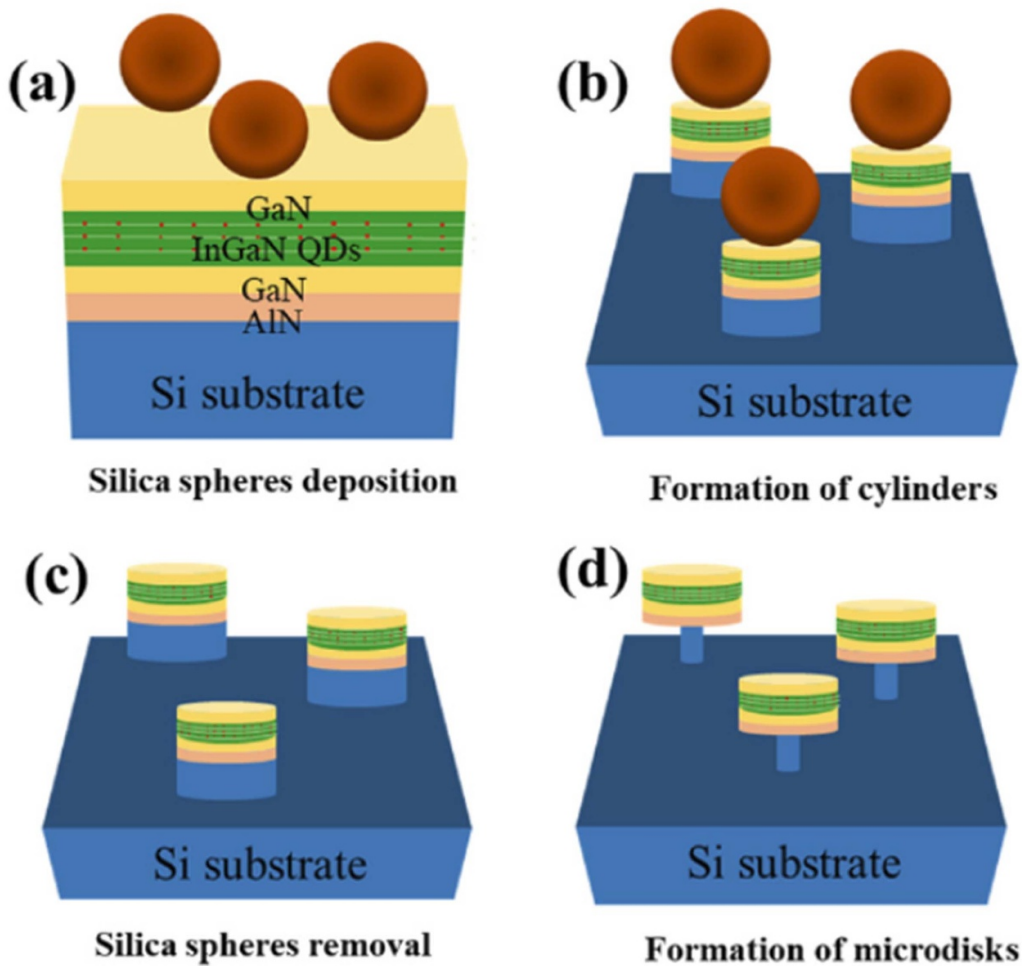
Figure 14. Schematic process flow of the microdisk lasers. (a) 1.0 μm silica sphere deposition; (b) ICP etching forms a cylinder mesa feature; (c) silica sphere removal; (d) wet etching forming the microdisks with a mushroom-shaped structure Reprinted from [181], with the permission of AIP Publishing.

QWs achieved a record-low lasing threshold of 6.2 μJ cm^{-2}, as shown in figure 15 [29]. As the pump volume decreases, the authors observed a systematic reduction in the lasing threshold of micro-rings.

Q Sun's group reported the initial observation of room-temperature electrically pumped lasing in an InGaN-based microdisk laser diode grown on Si in 2018 [182]. The detailed schematic structure of this InGaN micro-ring

Figure 15. (a) AFM images of uncapped InGaN epilayers on GaN. (b) Schematic showing the active layer composition. (c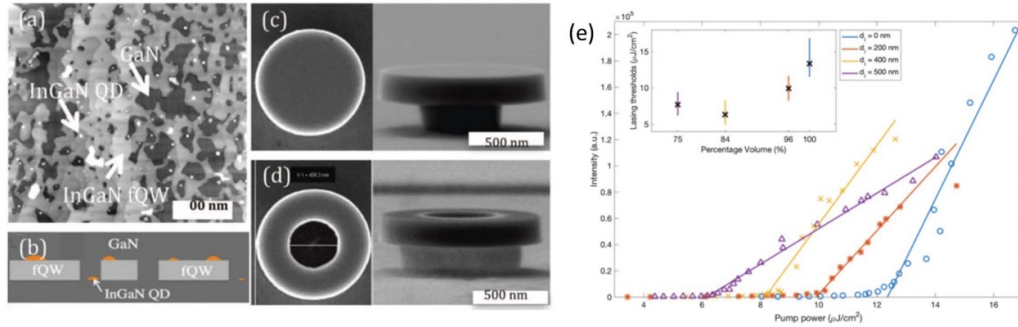) The top and side view SEM images of a microdisk and (d) a micro-ring with an inner diameter of 500 nm. (e) Spread of lasing thresholds in microdisks and micro-rings of different geometries. Reproduced from [29]. CC BY 4.0.
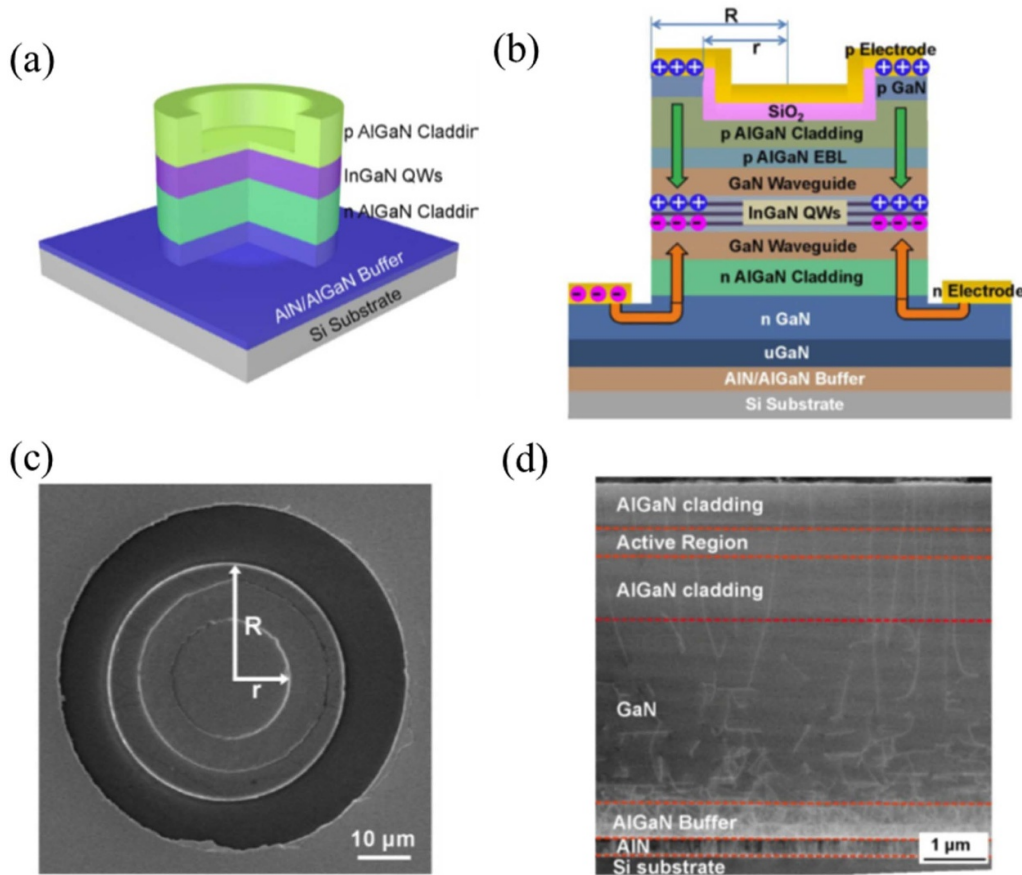

Figure 16. (a) Schematic architectures and (b) detailed schematic structure of an InGaN micro-ring laser grown on Si with AlGaN cladding layers. (c) Scanning electron microscopy and (d) transmission electron microscopy images of one as-fabricated InGaN micro-ring laser grown on Si. Reprinted with permission from [182]. © 2018 Optical Society of America.

laser grown on Si with AlGaN cladding layers is shown in figure 16. The InGaN-based microdisk lasers grown on Si are designed with a 'sandwich-like' architecture, utilizing upper and lower AlGaN cladding layers. This configuration was implemented to confine the optical field within the microdisk efficiently. The AlGaN cladding layers, possessing a lower refractive index than GaN, are crucial in confining the optical field from both the top and bottom directions.

Following the previous work, the authors advanced GaN-based near-UV microdisk laser diodes, achieving a lasing wavelength of 386.3 nm at room temperature [183]. To further mitigate thermal power, they reduced the radius of the microdisk laser to 8 μm [30]. As the device radius decreases from 20 to 8 μm, the thermal resistance increases from 146 to 437 K W^{-1}. Additionally, they significantly lowered the threshold current and junction temperature by reducing the

current injection area and device size [184]. Sun's group recently enhanced the performance of GaN-based microdisk lasers by implementing a SiO$_2$ passivation layer method [185]. They successfully demonstrated an initial on-chip integration of a GaN-based microring laser, waveguide, and photodetector on a Si substrate [186].

GaN-based microdisk lasers have emerged as a significant area of research owing to their compact size and low lasing thresholds, offering substantial potential for photonic and telecommunication applications. Recent advancements in fabrication techniques, such as PEC etching and the development of undercut structures, have enabled the successful demonstration of room-temperature lasing with exceptionally low thresholds. Innovations, including the integration of QD as active regions and the transfer of materials to Si substrates, have further enhanced the performance of these lasers. Ongoing research continues to address challenges related to lasing thresholds and thermal management, paving the way for the future of GaN microdisk laser technology.

6. Conclusions and prospects

This review summarizes the recent progress of III-nitride semiconductor lasers, particularly for four types of lasers, GaN-based EELs, VCSELs, PCSELs (or NCSELs), and WGM lasers. This review highlights the common goals of achieving high efficiency, high output power, and low lasing threshold across all laser types while also noting that the strategies and techniques employed vary depending on the specific laser type and intended application. Here we have discussed the different strategies and techniques for the different kinds of lasers. To elucidate the developmental trajectories of these lasers, this review consolidates and summarizes the outcomes of reported advancements in these four categories, as depicted in figure 17.

The successful commercialization of GaN-based EELs on GaN substrates has been achieved decades ago. Current research endeavors aim to explore the feasibility of utilizing cost-effective Si substrates, showcasing significant progress in advancing room-temperature CW electrically injected lasers on Si. This progress signifies the potential integration of GaN-based EELs with Si technologies. Despite these accomplishments, challenges persist, necessitating ongoing research to enhance the crystalline quality of GaN on Si substrates. The exploration of employing EELs in handheld pico-projection devices involved investigating reducing the cavity length to enhance the laser threshold, which was also reviewed.

This review also delves into the advancements in addressing design challenges and overcoming material quality obstacles in VCSELs. A key focus is the feasibility of extending VCSELs to longer wavelengths, particularly in the green spectrum. The discovery of low-threshold green VCSELs and the adoption of QD-based solutions present promising opportunities for the future evolution of VCSEL technology.

Advancements in GaN-based PCSELs hold promise for laser technology. Breakthroughs in nanofabrication and regrowth processes have resulted in improved performance metrics. Challenges persist, including precise fabrication and addressing uniformity issues through alternative methods. Recent developments in all-epitaxial green lasers exhibit promising features, and continued research is crucial for overcoming fabrication challenges and expanding applications, potentially revolutionizing laser design and functionality.

GaN-based microdisks, particularly with breakthroughs in PEC etching, demonstrate room-temperature CW blue WGM lasing with low thresholds. Various fabrication methods contribute to this progress, such as mushroom structures and direct growth on Si substrates. QDs offer solutions to high threshold issues, with GaN/AlN QD-based microdisks achieving record Q-factors and low thresholds. Recent advancements include room-temperature electrically pumped lasing on Si and optimizations in device architecture, with ongoing efforts focusing on further high-quality GaN on Si developments.
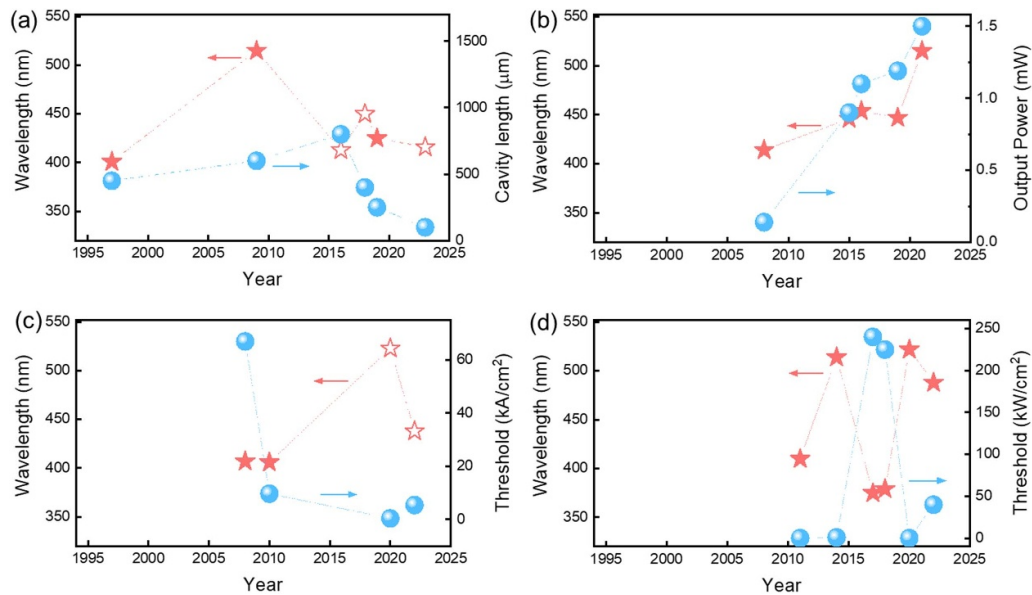
Figure 17. Selected of reported data of (a) cavity length and emission wavelength for CW-operated GaN-based EELs at room temperature by current injection (here solid stars represent lasers on GaN substrates and hollow stars represent on Si substrates) [10, 40, 47, 58, 63, 64]; (b) output power and emission wavelength for CW-operated GaN-based VCSELs at room temperature by current injection [25, 65, 83, 114, 115]; (c) lasing threshold current density and emission wavelength for GaN-based PCSELs or NCSELs at room temperature by current injection (solid stars represent lasers operated under pulsed operation and hollow stars represent CW operation) [26–28, 147]; (d) lasing threshold and emission wavelength for CW-operated optical pumped GaN-based WGM lasers [164, 171, 172, 179, 181, 187].

Data availability statement

All data that support the findings of this study are included within the article (and any supplementary files).

Acknowledgments

References

[1] Ichimura I, Maeda F, Osato K, Yamamoto K and Kasami Y 2000 Optical disk recording using a GaN blue-violet laser diode *Jpn. J. Appl. Phys.* **39** 937

[2] Nakamura S 1998 The roles of structural imperfections in InGaN-Based blue light-emitting diodes and laser diodes *Science* **281** 956–61

[3] Oubei H M *et al* 2015 4.8 Gbit/s 16-QAM-OFDM transmission based on compact 450-nm laser for underwater wireless optical communication *Opt. Express* **23** 23302–9

[4] Feneberg M, Leute R A R, Neuschl B, Thonke K and Bickermann M 2010 High-excitation and high-resolution photoluminescence spectra of bulk AlN *Phys. Rev. B* **82** 075208

[5] Monemar B, Paskov P P and Kasic A 2005 Optical properties of InN—the bandgap question *Superlattices Microstruct.* **38** 38–56

[6] Ju Z G *et al* 2013 Improved hole distribution in InGaN/GaN light-emitting diodes with graded thickness quantum barriers *Appl. Phys. Lett.* **102** 243504

[7] Tsai S-C, Lu C-H and Liu C-P 2016 Piezoelectric effect on compensation of the quantum-confined Stark effect in InGaN/GaN multiple quantum wells based green light-emitting diodes *Nano Energy* **28** 373–9

[8] Ju Z G, Tan S T, Zhang Z-H, Ji Y, Kyaw Z, Dikme Y, Sun X W and Demir H V 2012 On the origin of the redshift in the emission wavelength of InGaN/GaN blue light emitting diodes grown with a higher temperature interlayer *Appl. Phys. Lett.* **100** 123503

[9] Nakamura S N S 1991 GaN growth using GaN buffer layer *Jpn. J. Appl. Phys.* **30** L1705

[10] Sun Y *et al* 2016 Room-temperature continuous-wave electrically injected InGaN-based laser directly grown on Si *Nat. Photon.* **10** 595–9

[11] Oliver R A, Kappers M J, Sumner J, Datta R and Humphreys C J 2006 Highlighting threading dislocations in MOVPE-grown GaN using an *in situ* treatment with SiH$_4$ and NH$_3$ *J. Cryst. Growth* **289** 506–14

[12] Rhode S L, Fu W Y, Moram M A, Massabuau F C-P, Kappers M J, McAleese C, Oehler F, Humphreys C J, Dusane R O and Sahonta S L 2014 Structure and strain relaxation effects of defects in In$_x$Ga$_{1-x}$N epilayers *J. Appl. Phys.* **116** 103513

[13] Sun Q, Yan W, Feng M, Li Z, Feng B, Zhao H and Yang H 2016 GaN-on-Si blue/white LEDs: epitaxy, chip, and package *J. Semicond.* **37** 044006

[14] Amano H, Sawaki N, Akasaki I and Toyoda Y 1986 Metalorganic vapor phase epitaxial growth of a high quality GaN film using an AlN buffer layer *Appl. Phys. Lett.* **48** 353–5

[15] Amano H, Kito M, Hiramatsu K and Akasaki I 1989 P-type conduction in Mg-doped GaN treated with low-energy electron beam irradiation (LEEBI) *Jpn. J. Appl. Phys.* **28** L2112

[16] Nakamura S, Mukai T, Senoh M S M and Iwasa N I N 1992 Thermal annealing effects on P-type Mg-doped GaN films *Jpn. J. Appl. Phys.* **31** L139

[17] Nakamura S, Mukai T M T and Senoh M S M 1992 Si- and Ge-doped GaN films grown with GaN buffer layers *Jpn. J. Appl. Phys.* **31** 2883

[18] Nakamura S, Senoh M, Nagahama S-I, Iwasa N, Yamada T, Matsushita T, Kiyoku H K H and Sugimoto Y S Y 1996 InGaN-based multi-quantum-well-structure laser diodes *Jpn. J. Appl. Phys.* **35** L74

[19] Nakamura S *et al* 1998 Continuous-wave operation of InGaN/GaN/AlGaN-based laser diodes grown on GaN substrates *Appl. Phys. Lett.* **72** 2014–6

[20] Kishimoto K, Hirao T, Morizumi T, Nagao Y, Nakatsu Y, Yanamoto T and Nagahama S-I 2024 Development of highly efficient blue and green edge-emitting laser diodes *Proc. SPIE* **12886** 1288609

[21] Zhu D, Wallis D J and Humphreys C J 2013 Prospects of III-nitride optoelectronics grown on Si *Rep. Prog. Phys.* **76** 106501

[22] Murayama M, Nakayama Y, Yamazaki K, Hoshina Y, Watanabe H, Fuutagawa N, Kawanishi H, Uemura T and Narui H 2018 Watt-class green (530 nm) and blue (465 nm) laser diodes *Phys. Status Solidi* a **215** 1700513

[23] Hamaguchi T 2023 GaN-based VCSELs with a monolithic curved mirror: challenges and prospects *Photonics* **10** 470

[24] Nakatsu Y, Hirao T, Morizumi T, Nagao Y, Terao K, Nagai H, Masui S, Yanamoto T and Nagahama S-I 2023 Blue and green edge-emitting laser diodes and vertical-cavity surface emitting lasers on C-plane GaN substrates *Proc. SPIE* **12421** 124210F

[25] Yang T, Chen Y-H, Wang Y-C, Ou W, Ying L-Y, Mei Y, Tian A-Q, Liu J-P, Guo H-C and Zhang B-P 2023 Green vertical-cavity surface-emitting lasers based on InGaN quantum dots and short cavity *Nano-Micro. Lett.* **15** 223

[26] Matsubara H, Yoshimoto S, Saito H, Jianglin Y, Tanaka Y and Noda S 2008 GaN photonic-crystal surface-emitting laser at blue-violet wavelengths *Science* **319** 445–7

[27] Ra Y H, Rashid R T, Liu X, Sadaf S M, Mashooq K and Mi Z 2020 An electrically pumped surface-emitting semiconductor green laser *Sci. Adv.* **6** eaav7523

[28] Emoto K, Koizumi T, Hirose M, Jutori M, Inoue T, Ishizaki K, De Zoysa M, Togawa H and Noda S 2022 Wide-bandgap GaN-based watt-class photonic-crystal lasers *Commun. Mater.* **3** 72

[29] Wang D, Zhu T, Oliver R A and Hu E L 2018 Ultra-low-threshold InGaN/GaN quantum dot micro-ring lasers *Opt. Lett.* **43** 799–802

[30] Wang J, Feng M, Zhou R, Sun Q, Liu J, Sun X, Zheng X, Ikeda M, Sheng X and Yang H 2020 Continuous-wave electrically injected GaN-on-Si microdisk laser diodes *Opt. Express* **28** 12201–8

[31] Das A 2021 Recent developments in semipolar InGaN laser diodes *Semiconductors* **55** 272–82

[32] Najda S P *et al* 2022 GaN laser diode technology for visible-light communications *Electronics* **11** 1430

[33] Yang J *et al* 2024 GaN based ultraviolet laser diodes *J. Semicond.* **45** 011501

[34] Amano H, Tanaka T, Kunii Y, Kato K, Kim S T and Akasaki I 1994 Room-temperature violet stimulated emission from optically pumped AlGaN/GaInN double heterostructure *Appl. Phys. Lett.* **64** 1377–9

[35] Dingle R, Shaklee K L, Leheny R F and Zetterstrom R B 1971 Stimulated emission and laser action in gallium nitride *Appl. Phys. Lett.* **19** 5–7

[36] Khan M A, Krishnankutty S, Skogman R A, Kuznia J N, Olson D T and George T 1994 Vertical–cavity stimulated emission from photopumped InGaN/GaN heterojunctions at room temperature *Appl. Phys. Lett.* **65** 520–1

[37] Zubrilov A S, Nikolaev V I, Tsvetkov D V, Dmitriev V A, Irvine K G, Edmond J A and Carter C H Jr 1995 Spontaneous and stimulated emission from photopumped GaN grown on SiC *Appl. Phys. Lett.* **67** 533–5

[38] Itaya K *et al* 1996 Room temperature pulsed operation of nitride based multi-quantum-well laser diodes with cleaved facets on conventional C-face sapphire substrates *Jpn. J. Appl. Phys.* **35** L1315

[39] Kuramata A, Domen K, Soejima R, Horino K, Kubota S-I K S-I and Tanahashi T T T 1997 InGaN laser diode grown on 6H–SiC substrate using low-pressure metal organic vapor phase epitaxy *Jpn. J. Appl. Phys.* **36** L1130

[40] Nakamura S *et al* 1997 InGaN/GaN/AlGaN-based laser diodes with modulation-doped strained-layer superlattices *Jpn. J. Appl. Phys.* **36** L1568

[41] Nagahama S-I, Yanamoto T, Sano M and Mukai T 2001 Wavelength dependence of InGaN laser diode characteristics *Jpn. J. Appl. Phys.* **40** 3075

[42] Nam O-H, Bremser M D, Zheleva T S and Davis R F 1997 Lateral epitaxy of low defect density GaN layers via organometallic vapor phase epitaxy *Appl. Phys. Lett.* **71** 2638–40

[43] Usui A, Sunakawa H, Sakai A and Yamaguchi A A 1997 Thick GaN epitaxial growth with low dislocation density by hydride vapor phase epitaxy *Jpn. J. Appl. Phys.* **36** L899

[44] Avramescu A, Lermer T, Müller J, Eichler C, Bruederl G, Sabathil M, Lutgen S and Strauss U 2010 True green laser diodes at 524 nm with 50 mW continuous wave output power on c-plane GaN *Appl. Phys. Express* **3** 061003

[45] Enya Y *et al* 2009 531 nm green lasing of InGaN based laser diodes on semi-polar {2021} free-standing GaN substrates *Appl. Phys. Express* **2** 082101

[46] Hu L, Ren X, Liu J, Tian A, Jiang L, Huang S, Zhou W, Zhang L and Yang H 2020 High-power hybrid GaN-based green laser diodes with ITO cladding layer *Photon. Res.* **8** 279–85

[47] Miyoshi T, Masui S, Okada T, Yanamoto T, Kozaki T, Nagahama S-I and Mukai T 2009 510–515 nm InGaN-based green laser diodes on c-plane GaN substrate *Appl. Phys. Express* **2** 062201

[48] Miyoshi T, Masui S, Okada T, Yanamoto T, Kozaki T, Nagahama S-I and Mukai T 2010 InGaN-based 518 and 488 nm laser diodes on c-plane GaN substrate *Phys. Status Solidi* a **207** 1389–92

[49] Queren D, Avramescu A, Brüderl G, Breidenassel A, Schillgalies M, Lutgen S and Strauß U 2009 500 nm electrically driven InGaN based laser diodes *Appl. Phys. Lett.* **94** 081119

[50] Tian A *et al* 2016 Green laser diodes with low operation voltage obtained by suppressing carbon impurity in AlGaN: mg cladding layer *Phys. Status Solidi* c **13** 245–7

[51] Huang C-Y, Hardy M T, Fujito K, Feezell D F, Speck J S, DenBaars S P and Nakamura S 2011 Demonstration of 505 nm laser diodes using wavelength-stable semipolar (20-2-1) InGaN/GaN quantum wells *Appl. Phys. Lett.* **99** 241115

[52] Sizov D, Bhat R, Heberle A, Visovsky N and Zah C-E 2011 True-green (11–22) plane optically pumped laser with cleaved m-plane facets *Appl. Phys. Lett.* **99** 041117

[53] Yanashima K *et al* 2012 Long-lifetime true green laser diodes with output power over 50 mW above 525 nm grown on

semipolar {2021} GaN substrates *Appl. Phys. Express* **5** 082103

[54] Han X, Liu Y, Ren Y, Xing J, Zhu T, Wu Z, Liu Y and Zhang B 2019 Semipolar {11-22} InGaN/GaN multiple quantum well optically pumped laser diodes selectively grown on Si (111) substrates *Mater. Sci. Semicond. Process* **91** 327–32

[55] Kushimoto M, Tanikawa T, Honda Y and Amano H 2015 Optically pumped lasing properties of (1–101) InGaN/GaN stripe multiquantum wells with ridge cavity structure on patterned (001) Si substrates *Appl. Phys. Express* **8** 022702

[56] Murase T, Tanikawa T, Honda Y, Yamaguchi M and Amano H 2011 Optical properties of (1–101) InGaN/GaN MQW stripe laser structure on Si substrate *Phys. Status Solidi c* **8** 2160–2

[57] Feng M *et al* 2018 Room-temperature electrically injected AlGaN-based near-ultraviolet laser grown on Si *ACS Photonics* **5** 699–704

[58] Sun Y *et al* 2018 Room-temperature continuous-wave electrically pumped InGaN/GaN quantum well blue laser diode directly grown on Si *Light Sci. Appl.* **7** 13

[59] Zhou R *et al* 2020 InGaN-based lasers with an inverted ridge waveguide heterogeneously integrated on Si(100) *ACS Photonics* **7** 2636–42

[60] König H *et al* 2019 Visible GaN laser diodes: from lowest thresholds to highest power levels *Proc. SPIE* **10939** 109390C

[61] Becerra D L, Kuritzky L Y, Nedy J, Abbas A S, Pourhashemi A, Farrell R M, Cohen D A, DenBaars S P, Speck J S and Nakamura S 2016 Measurement and analysis of internal loss and injection efficiency for continuous-wave blue semipolar (20-2-1) III-nitride laser diodes with chemically assisted ion beam etched facets *Appl. Phys. Lett.* **108** 091106

[62] Farrell R M, Haeger D A, Hsu P S, Fujito K, Feezell D F, DenBaars S P, Speck J S and Nakamura S 2011 Determination of internal parameters for AlGaN-cladding-free m-plane InGaN/GaN laser diodes *Appl. Phys. Lett.* **99** 171115

[63] Zhang H, Shih C-W, Martin D, Caut A, Carlin J-F, Butté R and Grandjean N 2019 Short cavity InGaN-based laser diodes with cavity length below 300 μm *Semicond. Sci. Technol.* **34** 085005

[64] Kawaguchi Y, Murakawa K, Usagawa M, Aoki Y, Takeuchi K and Kamikawa T 2023 100 μm-cavity GaN-based edge emitting laser diodes by the automatic cleavage technique using GaN-on-Si epitaxial lateral overgrowth *Cryst. Growth Des.* **23** 3572–8

[65] Kuramoto M, Kobayashi S, Akagi T, Tazawa K, Tanaka K, Nakata K and Saito T 2019 Watt-class blue vertical-cavity surface-emitting laser arrays *Appl. Phys. Express* **12** 091004

[66] Iga K 2018 Forty years of vertical-cavity surface-emitting laser: invention and innovation *Jpn. J. Appl. Phys.* **57** 08PA01

[67] Iga K 2000 Surface-emitting laser-its birth and generation of new optoelectronics field *IEEE J. Sel. Top. Quantum Electron.* **6** 1201–15

[68] Iga K 2013 Vertical-cavity surface-emitting laser (VCSEL) *Proc. IEEE* **101** 2229–33

[69] Iga K 2008 Vertical-cavity surface-emitting laser: its conception and evolution *Jpn. J. Appl. Phys.* **47** 1

[70] Iga K, Koyama F and Kinoshita S 1988 Surface emitting semiconductor lasers *IEEE J. Quantum Electron.* **24** 1845–55

[71] Soda H, Iga K-I, Kitahara C and Suematsu Y 1979 GaInAsP/InP surface emitting injection lasers *Jpn. J. Appl. Phys.* **18** 2329–30

[72] Amann M C and Hofmann W 2009 InP-based long-wavelength VCSELs and VCSEL arrays *IEEE J. Sel. Top. Quantum Electron.* **15** 861–8

[73] Gierl C *et al* 2011 Surface micromachined tunable 1.55 μm-VCSEL with 102 nm continuous single-mode tuning *Opt. Express* **19** 17336–43

[74] Saxena D, Mokkapati S, Parkinson P, Jiang N, Gao Q, Tan H H and Jagadish C 2013 Optically pumped room-temperature GaAs nanowire lasers *Nat. Photon.* **7** 963–8

[75] Lei T, Ludwig K F and Moustakas T D 1993 Heteroepitaxy, polymorphism, and faulting in GaN thin films on silicon and sapphire substrates *J. Appl. Phys.* **74** 4430–7

[76] Liu L and Edgar J H 2002 Substrates for gallium nitride epitaxy *Mater. Sci. Eng. R* **37** 61–127

[77] Fortuna S A and Li X 2010 Metal-catalyzed semiconductor nanowires: a review on the control of growth directions *Semicond. Sci. Technol.* **25** 024005

[78] Kopf R F, Schubert E F, Downey S W and Emerson A B 1992 N- and P-type dopant profiles in distributed Bragg reflector structures and their effect on resistance *Appl. Phys. Lett.* **61** 1820–2

[79] Huang C-F, Chen C-Y, Lu C-F and Yang C C 2007 Reduced injection current induced blueshift in an InGaN∕GaN quantum-well light-emitting diode of prestrained growth *Appl. Phys. Lett.* **91** 051121

[80] Honda T, Katsube A, Sakaguchi T, Koyama F and Iga K I K 1995 Threshold estimation of GaN-based surface emitting lasers operating in ultraviolet spectral region *Jpn. J. Appl. Phys.* **34** 3527

[81] Redwing J M, Loeber D A S, Anderson N G, Tischler M A and Flynn J S 1996 An optically pumped GaN–AlGaN vertical cavity surface emitting laser *Appl. Phys. Lett.* **69** 1–3

[82] Lu T-C, Kao C-C, Kuo H-C, Huang G-S and Wang S-C 2008 CW lasing of current injection blue GaN-based vertical cavity surface emitting laser *Appl. Phys. Lett.* **92** 141102

[83] Higuchi Y, Omae K, Matsumura H and Mukai T 2008 Room-temperature CW lasing of a GaN-based vertical-cavity surface-emitting laser by current injection *Appl. Phys. Express* **1** 121102

[84] Omae K, Higuchi Y, Nakagawa K, Matsumura H and Mukai T 2009 Improvement in lasing characteristics of GaN-based vertical-cavity surface-emitting lasers fabricated using a GaN substrate *Appl. Phys. Express* **2** 052101

[85] Forman C A, Lee S, Young E C, Kearns J A, Cohen D A, Leonard J T, Margalith T, DenBaars S P and Nakamura S 2018 Continuous-wave operation of m-plane GaN-based vertical-cavity surface-emitting lasers with a tunnel junction intracavity contact *Appl. Phys. Lett.* **112** 111106

[86] Yamamoto S, Zhao Y, Pan C-C, Chung R B, Fujito K, Sonoda J, DenBaars S P and Nakamura S 2010 High-efficiency single-quantum-well green and yellow-green light-emitting diodes on semipolar (2021) GaN substrates *Appl. Phys. Express* **3** 122102

[87] Hamaguchi T *et al* 2019 Sub-milliampere-threshold continuous wave operation of GaN-based vertical-cavity surface-emitting laser with lateral optical confinement by curved mirror *Appl. Phys. Express* **12** 044004

[88] Nakajima H *et al* 2019 Single transverse mode operation of GaN-based vertical-cavity surface-emitting laser with monolithically incorporated curved mirror *Appl. Phys. Express* **12** 084003

[89] Kuramoto M, Kobayashi S, Akagi T, Tazawa K, Tanaka K, Saito T and Takeuchi T 2018 Enhancement of slope efficiency and output power in GaN-based vertical-cavity surface-emitting lasers with a SiO2-buried lateral index guide *Appl. Phys. Lett.* **112** 111104

[90] Holder C, Speck J S, DenBaars S P, Nakamura S and Feezell D 2012 Demonstration of nonpolar GaN-based vertical-cavity surface-emitting lasers *Appl. Phys. Express* **5** 092104

[91] Holder C O, Leonard J T, Farrell R M, Cohen D A, Yonkee B, Speck J S, DenBaars S P, Nakamura S and Feezell D F 2014 Nonpolar III-nitride vertical-cavity surface emitting lasers with a polarization ratio of 100% fabricated using photoelectrochemical etching *Appl. Phys. Lett.* **105** 031111

[92] Lu T-C, Chen S-W, Wu T-T, Tu P-M, Chen C-K, Chen C-H, Li Z-Y, Kuo H-C and Wang S-C 2010 Continuous wave operation of current injected GaN vertical cavity surface emitting lasers at room temperature *Appl. Phys. Lett.* **97** 071114

[93] Ng H M, Doppalapudi D, Iliopoulos E and Moustakas T D 1999 Distributed Bragg reflectors based on AlN/GaN multilayers *Appl. Phys. Lett.* **74** 1036–8

[94] Yao H H, Lin C F, Kuo H C and Wang S C 2004 MOCVD growth of AlN/GaN DBR structures under various ambient conditions *J. Cryst. Growth* **262** 151–6

[95] Zhu T, Dussaigne A, Christmann G, Pinquier C, Feltin E, Martin D, Butté R and Grandjean N 2008 Nonpolar GaN-based microcavity using AlN/GaN distributed Bragg reflector *Appl. Phys. Lett.* **92** 061114

[96] Bhattacharyya A, Iyer S, Iliopoulos E, Sampath A V, Cabalu J, Moustakas T D and Friel I 2002 High reflectivity and crack-free AlGaN/AlN ultraviolet distributed Bragg reflectors *J. Vac. Sci. Technol.* B **20** 1229–33

[97] Ji X-L, Jiang R-L, Xie Z-L, Liu B, Zhou J-J, Li L, Han P, Zhang R, Zheng Y-D and Gong H-M 2007 High-reflectivity AlGaN/AlN distributed Bragg reflector in ultraviolet region *Chin. Phys. Lett.* **24** 1735

[98] Xie Z L *et al* 2007 High reflectivity AlGaN/AlN DBR mirrors grown by MOCVD *J. Cryst. Growth* **298** 691–4

[99] Tao R, Arita M, Kako S, Kamide K and Arakawa Y 2015 Strong coupling in non-polar GaN/AlGaN microcavities with air-gap/III-nitride distributed Bragg reflectors *Appl. Phys. Lett.* **107** 101102

[100] Waldrip K E, Han J, Figiel J J, Zhou H, Makarona E and Nurmikko A V 2001 Stress engineering during metalorganic chemical vapor deposition of AlGaN/GaN distributed Bragg reflectors *Appl. Phys. Lett.* **78** 3205–7

[101] Chiu C H, Kuo H C, Lee C E, Lin C H, Cheng P C, Huang H W, Lu T C, Wang S C and Leung K M 2007 Fabrication and characteristics of thin-film InGaN–GaN light-emitting diodes with TiO_2/SiO_2 omnidirectional reflectors *Semicond. Sci. Technol.* **22** 831

[102] Huang H W, Lin C H, Yu C C, Lee B D, Kuo H C, Leung K M and Wang S C 2008 Investigation of InGaN/GaN power chip light emitting diodes with TiO_2/SiO_2 omnidirectional reflector *Semicond. Sci. Technol.* **23** 125006

[103] Lee W-C, Wang S-J, Uang K-M, Chen T-M, Kuo D-M, Wang P-R and Wang P-H 2011 Enhanced light output of vertical-structured GaN-based light-emitting diodes with TiO_2/SiO_2 reflector and roughened GaOx surface film *Jpn. J. Appl. Phys.* **50** 04DG06

[104] Someya T S T, Tachibana K T K, Lee J L J, Kamiya T K T and Arakawa Y A Y 1998 Lasing emission from an $In_{0.1}Ga_{0.9}N$ vertical cavity surface emitting laser *Jpn. J. Appl. Phys.* **37** L1424

[105] Wei-Hua C, Xiao-Dong H, Tao D, Rui L, Xue-Min Y, Tai-Ping Z, Wei-Min D, Zhi-Jian Y and Guo-Yi Z 2008 Influence of patterned TiO_2/SiO_2 dielectric multilayers for back and front mirror facets on GaN-based laser diodes *Chin. Phys. B* **17** 3363–6

[106] Huang G S, Chen H-G, Chen J R, Lu T C, Kuo H C and Wang S C 2007 Hybrid nitride microcavity using crack-free highly reflective AlN/GaN and Ta_2O_5/SiO_2 distributed Bragg mirrors *Phys. Status Solidi* a **204** 1977–81

[107] Kao C-C *et al* 2005 Fabrication and performance of blue GaN-based vertical-cavity surface emitting laser employing AlN/GaN and Ta_2O_5/SiO_2 distributed Bragg reflector *Appl. Phys. Lett.* **87** 081105

[108] Ma Y, Fan B, Chen Z, Lao Y, Yan L, Ma X, Zhuo Y, Pei Y and Wang G 2017 Enhanced light output of near-ultraviolet LEDs with Ta_2O_5/SiO_2 hybrid DBR reflector *IEEE Photon. Technol. Lett.* **29** 1564–7

[109] Kao T-T *et al* 2013 Sub-250 nm low-threshold deep-ultraviolet AlGaN-based heterostructure laser employing HfO_2/SiO_2 dielectric mirrors *Appl. Phys. Lett.* **103** 211103

[110] Réveret F *et al* 2016 High reflectance dielectric distributed Bragg reflectors for near ultra-violet planar microcavities: SiO_2/HfO_2 versus SiO_2/SiN_x *J. Appl. Phys.* **120** 093107

[111] Song Y-K, Zhou H, Diagne M, Ozden I, Vertikov A, Nurmikko A V, Carter-Coman C, Kern R S, Kish F A and Krames M R 1999 A vertical cavity light-emitting InGaN quantum well heterostructure *Appl. Phys. Lett.* **74** 3441–3

[112] Mei Y, Xu R-B, Xu H, Ying L-Y, Zheng Z-W, Zhang B-P, Li M and Zhang J 2018 A comparative study of thermal characteristics of GaN-based VCSELs with three different typical structures *Semicond. Sci. Technol.* **33** 015016

[113] Okur S *et al* 2013 GaN-based vertical cavities with all dielectric reflectors by epitaxial lateral overgrowth *Jpn. J. Appl. Phys.* **52** 08JH03

[114] Izumi S, Fuutagawa N, Hamaguchi T, Murayama M, Kuramoto M and Narui H 2015 Room-temperature continuous-wave operation of GaN-based vertical-cavity surface-emitting lasers fabricated using epitaxial lateral overgrowth *Appl. Phys. Express* **8** 062702

[115] Hamaguchi T, Fuutagawa N, Izumi S, Murayama M and Narui H 2016 Milliwatt-class GaN-based blue vertical-cavity surface-emitting lasers fabricated by epitaxial lateral overgrowth *Phys. Status Solidi* a **213** 1170–6

[116] Kuramoto M, Kobayashi S, Akagi T, Tazawa K, Tanaka K, Saito T and Takeuchi T 2018 High-output-power and high-temperature operation of blue GaN-based vertical-cavity surface-emitting laser *Appl. Phys. Express* **11** 112101

[117] Kuramoto M, Kobayashi S, Akagi T, Tazawa K, Tanaka K, Saito T and Takeuchi T 2019 High-power GaN-based vertical-cavity surface-emitting lasers with AlInN/GaN distributed Bragg reflectors *Appl. Sci.* **9** 416

[118] Zhao C, Tang C W, Lai B, Cheng G, Wang J and Lau K M 2020 Low-efficiency-droop InGaN quantum dot light-emitting diodes operating in the "green gap" *Photon. Res.* **8** 750–4

[119] Kasahara D, Morita D, Kosugi T, Nakagawa K, Kawamata J, Higuchi Y, Matsumura H and Mukai T 2011 Demonstration of blue and green GaN-based vertical-cavity surface-emitting lasers by current injection at room temperature *Appl. Phys. Express* **4** 072103

[120] Kenichi T, Hitoshi N, Daisuke M, Shingo M, Tomoya Y and Shin-ichi N 2021 Blue and green GaN-based vertical-cavity surface-emitting lasers with AlInN/GaN DBR *Proc. SPIE* **2021** 116860E

[121] Hamaguchi T *et al* 2020 Room-temperature continuous-wave operation of green vertical-cavity surface-emitting lasers with a curved mirror fabricated on {20−21} semi-polar GaN *Appl. Phys. Express* **13** 041002

[122] Mei Y, Weng G E, Zhang B P, Liu J P, Hofmann W, Ying L Y, Zhang J Y, Li Z C, Yang H and Kuo H C 2017 Quantum

dot vertical-cavity surface-emitting lasers covering the 'green gap' *Light Sci. Appl.* **6** e16199

[123] John S 1987 Strong localization of photons in certain disordered dielectric superlattices *Phys. Rev. Lett.* **58** 2486–9

[124] Yablonovitch E 1987 Inhibited spontaneous emission in solid-state physics and electronics *Phys. Rev. Lett.* **58** 2059–62

[125] Yablonovitch E and Gmitter T J 1989 Photonic band structure: the face-centered-cubic case *Phys. Rev. Lett.* **63** 1950–3

[126] Yablonovitch E, Gmitter T J and Leung K M 1991 Photonic band structure: the face-centered-cubic case employing nonspherical atoms *Phys. Rev. Lett.* **67** 2295–8

[127] Yablonovitch E, Gmitter T J, Meade R D, Rappe A M, Brommer K D and Joannopoulos J D 1991 Donor and acceptor modes in photonic band structure *Phys. Rev. Lett.* **67** 3380–3

[128] Painter O, Lee R K, Scherer A, Yariv A, O'Brien J D, Dapkus P D and Kim I 1999 Two-dimensional photonic band-gap defect mode laser *Science* **284** 1819–21

[129] Park H-G, Kim S-H, Kwon S-H, Ju Y-G, Yang J-K, Baek J-H, Kim S-B and Lee Y-H 2004 Electrically driven single-cell photonic crystal laser *Science* **305** 1444–7

[130] Akahane Y, Asano T, Song B-S and Noda S 2003 High-Q photonic nanocavity in a two-dimensional photonic crystal *Nature* **425** 944–7

[131] Johnson S G, Fan S, Mekis A and Joannopoulos J D 2001 Multipole-cancellation mechanism for high-Q cavities in the absence of a complete photonic band gap *Appl. Phys. Lett.* **78** 3388–90

[132] Srinivasan K and Painter O 2002 Momentum space design of high-Q photonic crystal optical cavities *Opt. Express* **10** 670–84

[133] Vučković J, Lončar M, Mabuchi H and Scherer A 2001 Design of photonic crystal microcavities for cavity QED *Phys. Rev. E* **65** 016608

[134] Choi Y-S, Hennessy K, Sharma R, Haberer E, Gao Y, DenBaars S P, Nakamura S, Hu E L and Meier C 2005 GaN blue photonic crystal membrane nanocavities *Appl. Phys. Lett.* **87** 243101

[135] Khare R and Hu E L 1991 Dopant selective photoelectrochemical etching of GaAs homostructures *J. Electrochem. Soc.* **138** 1516–9

[136] Minsky M S, White M and Hu E L 1996 Room-temperature photoenhanced wet etching of GaN *Appl. Phys. Lett.* **68** 1531–3

[137] Stonas A R, Kozodoy P, Marchand H, Fini P, DenBaars S P, Mishra U K and Hu E L 2000 Backside-illuminated photoelectrochemical etching for the fabrication of deeply undercut GaN structures *Appl. Phys. Lett.* **77** 2610–2

[138] Stonas A R, MacDonald N C, Turner K L, DenBaars S P and Hu E L 2001 Photoelectrochemical undercut etching for fabrication of GaN microelectromechanical systems *J. Vac. Sci. Technol. B* **19** 2838–41

[139] Tamboli A C, Schmidt M C, Rajan S, Speck J S, Mishra U K, DenBaars S P and Hu E L 2009 Smooth top-down photoelectrochemical etching of m-plane GaN *J. Electrochem. Soc.* **156** H47–H51

[140] Zhao C, Zhang X, Tang C W, Wang J and Lau K M 2020 Selective lateral photoelectrochemical wet etching of InGaN nanorods *J. Vac. Sci. Tech. B* **38** 060602

[141] Imada M, Chutinan A, Noda S and Mochizuki M 2002 Multidirectionally distributed feedback photonic crystal lasers *Phys. Rev. B* **65** 195306

[142] Kaminow I P, Weber H P and Chandross E A 1971 Poly(methyl methacrylate) dye laser with internal diffraction grating resonator *Appl. Phys. Lett.* **18** 497–9

[143] Kogelnik H and Shank C V 1971 Stimulated emission in a periodic structure *Appl. Phys. Lett.* **18** 152–4

[144] Ogawa S, Imada M, Yoshimoto S, Okano M and Noda S 2004 Control of light emission by 3D photonic crystals *Science* **305** 227–9

[145] Weng P H, Wu T T and Lu T C 2012 Study of band-edge modes in GaN-based photonic crystal surface-emitting lasers by the multiple-scattering method *IEEE J. Sel. Top. Quantum Electron.* **18** 1629–35

[146] Wu T T, Chen C C and Lu T C 2015 Effects of lattice types on GaN-based photonic crystal surface-emitting lasers *IEEE J. Sel. Top. Quantum Electron.* **21** 426–31

[147] Kawashima S, Kawashima T, Nagatomo Y, Hori Y, Iwase H, Uchida T, Hoshino K, Numata A and Uchida M 2010 GaN-based surface-emitting laser with two-dimensional photonic crystal acting as distributed-feedback grating and optical cladding *Appl. Phys. Lett.* **97** 251112

[148] Lu T-C, Chen S-W, Lin L-F, Kao T-T, Kao C-C, Yu P, Kuo H-C, Wang S-C and Fan S 2008 GaN-based two-dimensional surface-emitting photonic crystal lasers with AlN/GaN distributed Bragg reflector *Appl. Phys. Lett.* **92** 011129

[149] Wu T T, Chen H W, Lan Y P, Lu T C and Wang S C 2014 Suspended GaN-based band-edge type photonic crystal nanobeam cavities *Opt. Express* **22** 2317–23

[150] Vafadar M F and Zhao S 2023 Ultralow threshold surface emitting ultraviolet lasers with semiconductor nanowires *Sci. Rep.* **13** 6633

[151] Vafadar M F and Zhao S 2024 Architecture for surface-emitting lasers with on-demand lasing wavelength by nanowire optical cavities *ACS Nano* **18** 14290–7

[152] McCall S L, Levi A F J, Slusher R E, Pearton S J and Logan R A 1992 Whispering-gallery mode microdisk lasers *Appl. Phys. Lett.* **60** 289–91

[153] Mohideen U, Slusher R E, Jahnke F and Koch S W 1994 Semiconductor microlaser linewidths *Phys. Rev. Lett.* **73** 1785–8

[154] Si Z *et al* 2023 The effect of lateral growth of self-assembled GaN microdisks on UV lasing action *Nano Res.* **16** 11096–106

[155] Vahala K J 2003 Optical microcavities *Nature* **424** 839–46

[156] Gao Y, Ben-Yaacov I, Mishra U and Hu E 2011 Etched aperture GaN cavet through photoelectrochemical wet etching *Int. J. High Speed Electron. Syst.* **14** 245–64

[157] Gao Y, Craven M D, Speck J S, Baars S P D and Hu E L 2004 Dislocation- and crystallographic-dependent photoelectrochemical wet etching of gallium nitride *Appl. Phys. Lett.* **84** 3322–4

[158] Haberer E D, Sharma R, Meier C, Stonas A R, Nakamura S, DenBaars S P and Hu E L 2004 Free-standing, optically pumped, GaN/InGaN microdisk lasers fabricated by photoelectrochemical etching *Appl. Phys. Lett.* **85** 5179–81

[159] Stonas A R, Margalith T, DenBaars S P, Coldren L A and Hu E L 2001 Development of selective lateral photoelectrochemical etching of InGaN/GaN for lift-off applications *Appl. Phys. Lett.* **78** 1945–7

[160] Tamboli A C, Hirai A, Nakamura S, DenBaars S P and Hu E L 2009 Photoelectrochemical etching of p-type GaN heterostructures *Appl. Phys. Lett.* **94** 151113

[161] Tamboli A C, Haberer E D, Sharma R, Lee K H, Nakamura S and Hu E L 2006 Room-temperature continuous-wave lasing in GaN/InGaN microdisks *Nat. Photon.* **1** 61

[162] Tajiri T, Sosumi S, Shimoyoshi K and Uchida K 2023 Fabrication and optical characterization of GaN micro-disk cavities undercut by laser-assisted photo-electrochemical etching *Jpn. J. Appl. Phys.* **62** SC1069

[163] Kouno T, Sakai M, Kishino K and Hara K 2013 Optically pumped lasing action with unusual wavelength of approximately 390 nm in hexagonal GaN microdisks fabricated by radio-frequency plasma-assisted molecular beam epitaxy *Jpn. J. Appl. Phys.* **52** 04CH07

[164] Fletcher P, Martínez de Arriba G, Tian Y, Poyiatzis N, Zhu C, Feng P, Bai J and Wang T 2022 Optical characterisation of InGaN-based microdisk arrays with nanoporous GaN/GaN DBRs *J. Appl. Phys.* **55** 464001

[165] Mei Y, Xie M, Long H, Ying L and Zhang B 2022 Low threshold GaN-based microdisk lasers on silicon with high Q factor *J. Lightwave Technol.* **40** 2952–8

[166] Zhang X, Li Z, Zhang Y, Wang X, Yi X, Wang G and Li J 2022 Heterogeneously integrated InGaN-based green microdisk light-emitters on Si (100) *Opt. Express* **30** 26676–89

[167] Gu P, Yang S, Ma L, Yang T, Hou X, Mei Y, Ying L, Long H and Zhang B 2023 Flexible GaN-based ultraviolet microdisk lasers on PET substrate *Opt. Lett.* **48** 4117–20

[168] Choi H W, Hui K N, Lai P T, Chen P, Zhang X H, Tripathy S, Teng J H and Chua S J 2006 Lasing in GaN microdisks pivoted on Si *Appl. Phys. Lett.* **89** 211101

[169] Sellés J *et al* 2016 III-Nitride-on-silicon microdisk lasers from the blue to the deep ultra-violet *Appl. Phys. Lett.* **109** 231101

[170] Zhang X, Cheung Y F, Zhang Y and Choi H W 2014 Whispering-gallery mode lasing from optically free-standing InGaN microdisks *Opt. Lett.* **39** 5614–7

[171] Zhu G, Li J, Li J, Guo J, Dai J, Xu C and Wang Y 2018 Single-mode ultraviolet whispering gallery mode lasing from a floating GaN microdisk *Opt. Lett.* **43** 647–50

[172] Athanasiou M, Smith R, Liu B and Wang T 2014 Room temperature continuous–wave green lasing from an InGaN microdisk on silicon *Sci. Rep.* **4** 7250

[173] Athanasiou M, Smith R M, Pugh J, Gong Y, Cryan M J and Wang T 2017 Monolithically multi-color lasing from an InGaN microdisk on a Si substrate *Sci. Rep.* **7** 10086

[174] Englund D, Fattal D, Waks E, Solomon G, Zhang B, Nakaoka T, Arakawa Y, Yamamoto Y and Vučković J 2005 Controlling the spontaneous emission rate of single quantum dots in a two-dimensional photonic crystal *Phys. Rev. Lett.* **95** 013904

[175] Wan Y *et al* 2017 Monolithically integrated InAs/InGaAs quantum dot photodetectors on silicon substrates *Opt. Express* **25** 27715–23

[176] Zhao C, Tang C W, Cheng G, Wang J and Lau K M 2020 InGaN quantum dots with short exciton lifetimes grown on polar c-plane by metal-organic chemical vapor deposition *Mater. Res. Express* **7** 115903

[177] Wan Y *et al* 2017 13 μm submilliamp threshold quantum dot micro-lasers on Si *Optica* **4** 940–4

[178] Zhang M, Banerjee A, Lee C-S, Hinckley J M and Bhattacharya P 2011 A InGaN/GaN quantum dot green (λ=524 nm) laser *Appl. Phys. Lett.* **98** 221104

[179] Mexis M *et al* 2011 High quality factor nitride-based optical cavities: microdisks with embedded GaN/Al(Ga)N quantum dots *Opt. Lett.* **36** 2203–5

[180] Aharonovich I, Woolf A, Russell K J, Zhu T, Niu N, Kappers M J, Oliver R A and Hu E L 2013 Low threshold, room-temperature microdisk lasers in the blue spectral range *Appl. Phys. Lett.* **103** 021112

[181] Zhao C, Tang C W, Wang J and Lau K M 2020 Ultra-low threshold green InGaN quantum dot microdisk lasers grown on silicon *Appl. Phys. Lett.* **117** 031104

[182] Feng M *et al* 2018 Room-temperature electrically pumped InGaN-based microdisk laser grown on Si *Opt. Express* **26** 5043–51

[183] Wang J *et al* 2019 GaN-based ultraviolet microdisk laser diode grown on Si *Photon. Res.* **7** B32–B35

[184] Wang J, Feng M, Zhou R, Sun Q, Liu J, Sun X, Zheng X, Sheng X and Yang H 2020 Thermal characterization of electrically injected GaN-based microdisk lasers on Si *Appl. Phys. Express* **13** 074002

[185] Zhao H, Feng M, Liu J, Sun X, Li Y, Wu X, Liu Q, Yilmaz E, Sun Q and Yang H 2023 Performance improvement of GaN-based microdisk lasers by using a PEALD-SiO$_2$ passivation layer *Opt. Express* **31** 20212–20

[186] Zhao H, Feng M, Liu J, Sun X, Tao T, Sun Q and Yang H 2023 Unidirectional emission of GaN-on-Si microring laser and its on-chip integration *Nanophotonics* **12** 111–8

[187] Zhu G Y, Qin F F, Guo J Y, Xu C X and Wang Y J 2017 Unidirectional ultraviolet whispering gallery mode lasing from floating asymmetric circle GaN microdisk *Appl. Phys. Lett.* **111** 202103